LAWRENCE
LIVERMORE
NATIONAL
LABORATORY

LLNL-TR-855777

The National Diagnostic Plan (NDP) for HED Science September 2023

J. S. Ross

October 10, 2023

Disclaimer

This work performed under the auspices of the U.S. Department of Energy by Lawrence Livermore National Laboratory under Contract DE-AC52-07NA27344.

The National Diagnostic Plan (NDP) for HED Science September 2023

Abstract: This documents the National Diagnostic Plan as of September 2023. The major changes in this version compared to the NDP document issued in 2021 are the new schedules and the text for the national transformative diagnostics - section III. The many local diagnostics for our three Inertial Confinement Fusion (ICF) facilities; NIF, Z and OMEGA are updated and captured in section V.

Summary: The National Nuclear Security Administration (NNSA) has made significant investments in major facilities and high-performance computing to successfully execute the Stockpile Stewardship Program (SSP). The more information obtained about the physical state of the plasmas produced, the more stringent the test of theories, models, and codes can be, leading to increased confidence in our predictive capability. To respond to the increasing sophistication of the ICF program, a multi-year program to develop and deploy advanced diagnostics has been developed by the expert scientific community. To formalize these previously collegial activities NNSA directed the formation and duties of the National Diagnostics Working Group (NDWG) for HED Science.

The NDWG has identified nine transformational diagnostics, shown in Table 1, that will provide unprecedented information from experiments in support of the SSP at NIF, Z and OMEGA. Table 2 shows how the missions of the SSP experiments including materials, complex hydrodynamics, radiation flow and effects and thermo-nuclear burn and boost will produce new observables, which need to be measured using a variety of the largely new diagnostic technologies used in the ten transformational diagnostics. The data provided by these diagnostics will validate and improve the physics contained within the SSP's simulations and both uncover and quantify important phenomena that lie beyond our present understanding.

Transformative diagnostic	Collaborating Institutions	New capability
Pulse Dilation Imaging w/hCMOS (SLOS, DIXI, HYXI)	**SNL, GA, LLNL, LLE**	**Multi-dimensional shape and spectra with unprecedented time and space resolution for fusion, Pu strength, and radiation effects sources**
Ultraviolet Thomson Scattering (UVTS)	**LLE, LLNL, LANL, NRL**	**Localized plasma conditions and turbulence in hohlraums and Laser Direct Drive ablation plasma. Additional uses include plasma conditions at low density for rad flow studies and many discovery science applications.**
3D n/gamma imaging (NIS)	**LANL, LLNL, SNL**	**3D shape & size of both burning and cold compressed fuel, as well as remaining carbon ablator**
Gamma spectroscopy (GCD/GRH)	**LANL, AWE, GA, LLNL, SNL, NNSS**	**Fusion burn history allowing inferred pressure with increased precision and measured truncation of burn from degradation mechanisms such as mix and loss of confinement.**
Time resolved neutron spectrum (MRS-time)	**MIT, LLNL, GA, LLE**	**Time evolution of the fusion burn temperature and areal density**
Time resolved diffraction (XRDt)	**SNL, LLNL, LLE**	**Time evolution of material structure (including weapon materials) and compression at high pressure. Also enables more efficient facility use through multiple measurements on a single shot.**

High Resolution Velocimeter (HRV)	**LLNL, LLE, SNL**	**High resolution line-imaging velocimetry measurements including higher accuracy (<1%) material EOS at high pressure. Also enables more efficient facility use through multiple high-fidelity measurements on a single shot.**
>15 keV X-ray detection (DHEX)	**LLNL, LLE, SNL**	**Multiple-frame time resolved detection of high energy (>15 keV) x-rays with high detection efficiency.**
hCMOS	**SNL, LLNL**	**Multi-frame, burst mode imaging sensor capable of capturing images on the nanosecond timescale and nanosecond gated single frame radiation hardened image sensors.**

Table 1: The ten transformational diagnostics, institutional involvement & capability.

Mission	New Observable	Technique	Acronym
Materials	**Strength vs time of compressed Pu**	**>4 images/costly target**	**SLOS, hCMOS**
	Phase change of compressed Pu - rates	**Time resolved x-ray diffraction**	**XRDt**
	EOS of compressed Pu	**High resolution VISAR velocimetry**	**HRV**
Hydro and Properties	**High energy x-ray images of Structure**	**Detection of High Energy x-rays**	**DHEX**
	T_e of Marshak wave	**Deep U.V. Thomson Scattering**	**UVTS**
Outputs and Survivability	**Hard spectrum vs space & time**	**SLOS**	**hCMOS**
TN Burn and Pursuit of High Yield	**Time history of burn**	**Ultra-fast Cerenkov detector**	**GCD**
	3D T_e and density vs time	**Dilation tube +SLOS +Wolter**	**SLOS, hCMOS**
	3D burn, 3D mix vs time	**3D neutron/γ imaging**	**NIS**
	T_{ion} and areal density vs time	**Neutron spectrum vs time**	**MRS-time**
All	**Hohlraum density & T vs space & time**	**Deep U.V. Thomson Scattering**	**UVTS**

Table 2: How the missions of the SSP will be enhanced by new observables measured by the ten transformational diagnostics being developed under the guidance of the NDWG.

In addition to the transformational diagnostics, there are:

(1) a set of broad diagnostics coordinated across the ICF sites,
(2) a large number of local diagnostics associated with the three large facilities: NIF, Z and OMEGA.

This document is an update of the NDP as of 9/21/2022. The activities of the NDWG and its organization and leadership are summarized in section II. The organization, progress, and plans for the transformational diagnostics are in section III. The activities of the broad diagnostics are in section IV. Finally, the progress and plans for the local diagnostics on NIF, Z and OMEGA are in section V.

II: Recent activities of the National Diagnostic Working Group (NDWG)

IIa: ICF and HED Diagnostics: Background and Mission

ICF and High Energy Density (HED) physics experiments involve phenomena that occur on timescales measured in picoseconds and spatial scales measured in micrometers (or microns). Observable information is conveyed in photons with energies ranging from visible light to MeV gamma rays, and in charged and neutral

particles from fusion reactions. Progress in ICF and HED has been dependent for decades on the development and innovation of new instruments and techniques to measure the observables with increasing temporal, spatial, and energy resolution, and with the ability to gather more data in a single experiment.

Since 2008 there have been regular NDWG meetings, initially to foster national participation in the diagnostics for the NIF and recently to coordinate research and development of HED diagnostics across the ICF sites for NIF, Z and OMEGA. ***By coordinating efforts, each site is able to capitalize on the advances made at the other sites, share expertise, and incorporate new techniques into their own programs.***

The national diagnostics development effort is divided into three groups:

- Transformational Diagnostics: diagnostics requiring a major national effort with the potential to transform experimental capability for the most critical science needs across the complex.
- Broad Diagnostics: diagnostic efforts and techniques requiring significant national efforts which will enable new or more precise measurements across the complex.
- Local Diagnostics: important diagnostics that implement known technology for a local need and are identified by facility management responding to the needs of the local user community.

The NNSA ICF and HED programs supports stockpile stewardship through the four principal missions shown in Table 2. The facilities also support National Security Applications (NSA) with other national agencies and basic science conducted mainly in collaboration with universities. The decisions on which new diagnostics to develop depends on a combination of the diagnostic usage at the various facilities, the prioritized needs of the programs, the status of technology, and the requests from the user community. Each facility has a different process for making these decisions for local diagnostics. For transformational and broad diagnostics, the development activities are prioritized, advocated for, and concerns are raised as appropriate by the appointed leaders of the NDWG. The core leadership of the NDWG as appointed by the ICF Execs are James Steven Ross (Lawrence Livermore National Lab, LLNL), Sean Regan (Laboratory for Laser Energetics, LLE), Eric Harding (Sandia National Laboratories, SNL), and Eric Loomis (Los Alamos National Laboratory, LANL) with consistent support from Joe Kilkenny (General Atomics, GA), Perry Bell, Doug Larson and Dave Bradley (LLNL), Johan Frenje (Massachusetts Institute of Technology, MIT), Chuck Sorce and Steven Ivancic (LLE), Michael Jones (SNL), and John Kline and Ann Satsangi (LANL).

IIb: Recent activities and organization of the NDWG

(i) The Dec. 2022 NDWG meeting was hosted by Sandia National Laboratory. A total of 93 in-person participants and 28 virtual participants representing institutions from around the world came together to discuss diagnostic development and progress.
(ii) The NDWG leadership group met via video teleconference in Feb 2023 to review progress.
(iii) The NDWG leadership group met via Hybrid meeting / video teleconference at LLNL in May 2022 to review progress.
(iv) The NDWG leadership group met via video teleconference in August 2023 to review progress and re-plan technical progress according to the expected budget for FY23. This document includes new updates based on the plan formulated during that meeting.
(v) On December 5th, 2022, a NIF DT experiment produced a yield exceeding 3 MJ, the first NIF experiment to achieve a gain greater than 1. Understanding this class of experiment and its impact on diagnostic needs continues to be a focus of the NDWG.

III: Transformational Diagnostics

Section IIIa is an overview of the transformational diagnostics. Section IIIb is a summary of the achievements and plans for each of the transformational diagnostics.

IIIa: Overview of the Transformational Diagnostics

The NDWG defined Transformational Diagnostics as those requiring a major national effort with the potential to transform experimental capability for the most critical science needs across the complex. In early 2015 a set of eight transformational diagnostics were identified. This set of diagnostics was reviewed by an independent group of experts in 2015 who reported to NNSA on the relative merit and urgency of each proposed capability (report is available). The NDWG monitors, on a quarterly basis, progress on these transformational diagnostics, as described in section II, and makes recommendations to the sites in terms of development priority and resource requirements. As diagnostics are commissioned and work is completed, that diagnostic is no longer tracked as part of the NDP. New diagnostics are added by agreement of the NDWG Leadership. There is a simplified description of these diagnostics starting on page 41 of NNSA's 2016 Inertial Confinement Fusion Program Framework DOE/NA-0044, and in Appendix C.

Each category of transformational diagnostics can mean many actual diagnostics at some or all three of the major facilities. The plans for implementation consist of many phases. Table 3 is the updated top-level schedule for the transformative diagnostics as of September 2022. More details are in Section IIIb. These schedules are largely consistent with the expected budgets but can be affected by both the implemented annual site allocations by NNSA and the distributions relative to other funding priorities by each of the site managers.

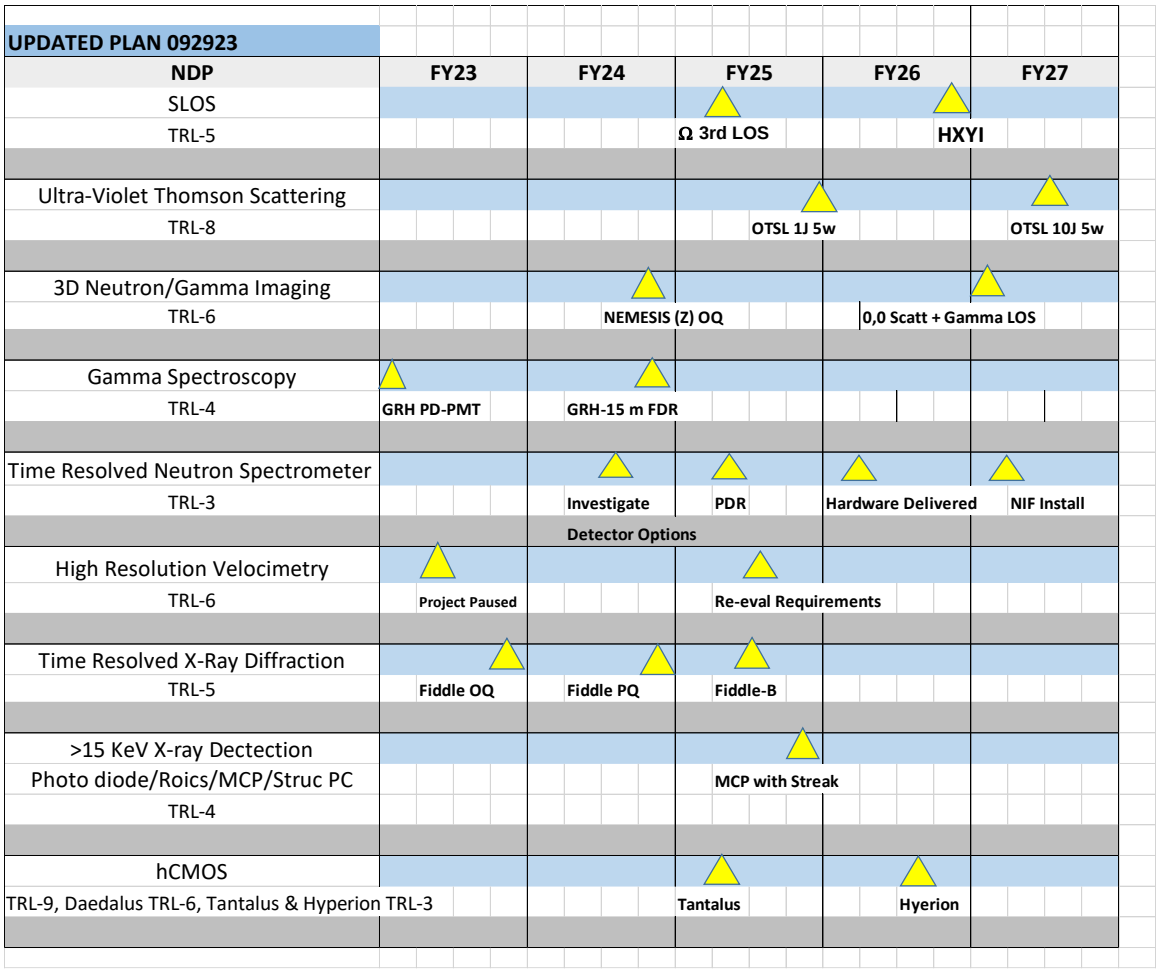

Table 3: Schedule for the transformational diagnostics. The acronym definition is below.

SLOS1 – 4-frame SLOS built for use in a manipulator on NIF that will be used with pinholes and then the Crystal Backlit Imager (section V-1).

TRL – Technical readiness level on a scale of 1-9 with 9 being further developed (details in the appendix).

HSLOS – A neutron Hardened Single Line of Sight detector consisting of a time dilation tube in front of a hCMOS detector.

Ω SLOS-TRXI-2 third line-of-sight for x-ray imaging on OMEGA consisting of a time dialation tube in front of a hCMOS detector

HE-hCMOS – hCMOS cameras with enhanced sensitivity to high energy x-rays using GaAs diode material.

6-fm hCMOS – upgraded hCMOS sensor with more frames and faster time resolution.

DD Bkgnd – Measurement of Direct Drive background plasma light emission level

HOHLR-1J, 5w – 5w Optical Thomson Scattering from a hohlraum or a Direct Drive plasma early in a shaped "ignition" pulse.

Hohlraum-10J, 5w – 5w Optical Thomson Scattering from a hohlraum during the main laser pulse of ignition-relevant targets

90,315 Un-scattered LOS – Imaging of un-scattered neutrons on 90,315 line-of-sight.

90,315 Scattered LOS - Imaging of scattered neutrons on 90,315 line-of-sight.

0,0 Scattered LOS – Imaging of down-scattered neutrons from (near) the north pole.

20ps TDT in well – Time history of gamma ray emission using the Time Dilation Detector in a well at 3.9 m from target chamber center.
High Sens./high dynamic range GCD – Time history of gamma ray emission at ~1 m from target chamber center
NIF Foil Test—Test of higher efficiency by mounting conversion foil on NIF hohlraum.
Wolter-Z – First implementation of Wolter optics on Z for >15 keV x-ray source shape.
Ag-Wolter – Wolter optic on Z tailored for Ag spectral line emission
MRSt NIF - Time resolved Magnetic Recoil Spectrometer on NIF
NIFt - A time resolving curved crystal spectrometer on NIF (dHiRes) in front of an x-ray streak camera.
NIF EXAFS Pu – A focusing, high resolution crystal spectrometer to perform Extended X-ray Absorption Fine Structure (EXAFS) spectroscopy through compressed plutonium
Toroidal-NIF – Toroidal optics for high resolution spatial distribution of hot spot electron temperature on NIF.
Streaked Omega – Phase and compression evolution using x-ray streak camera measurements on Omega.
HRV – High Resolution Velocimeter diagnostic
G3D – Coupled hCMOS cameras to NIF diffraction platform for multi-frame phase.
Z-High E – Single frame diffraction on Z at >10 keV
NIF ph2 – Coupled time dilation tube to hCMOS NIF diffraction platform for multi-frame high speed diffraction.
Daedalus V2: Next generation ROIC with tiling capability and deeper electron well for extended spectral range for spectroscopy.
Tantalus: First ROIC to be manufactured in an external foundry with integration times of around 500ps. Keystone for commercialization.
SFS: Single Frame Sensor a hCMOS sensor with <500ps temporal resolution (now named Hyperion)
HYXI: High Yield X-ray Imager a hCMOS based pulse dilation imager for x-ray hot spot self-emission for use on 10MJ+ NIF experiments.

IIIb: Achievements and plans for each of the nine transformational diagnostics.

IIIb-1: Single Line-of-Sight (SLOS) Imaging

Two key technologies developed within the ICF program are revolutionizing gated x-ray detectors. These technologies are pulse-dilation tubes developed in collaboration between General Atomics, Kentech Instruments, and LLNL, and fast-gated hybrid complementary metal-oxide-semiconductor (hCMOS) sensors developed at SNL. The scope of the hCMOS development has caused this effort to be covered in a new section specifically addressing hCMOS ROICs and diodes, see hCMOS section. Pulse-dilation coupled with hCMOS sensors provides a transformative capability of time gating for multiple frames along a single line-of-sight (SLOS) at gate times as short as 10 ps. Used on its own, the hCMOS sensor can provide direct detection of multi-keV x-rays or electrons at gate times ≥ 1 ns as well as visible to near IR laser beams. Pulse-dilation SLOS framing cameras are transformative because they enable multiple time-gated detection of x-ray images or spectra at frame rates never before possible. Spectra are recorded using curved crystals. Images are recorded with curved crystals or multi-layer mirror optics, which can have

superior spatial resolution and energy selectivity over pinhole/slit optics, but are too expensive or take up too much space to create an array of many images along many lines-of-sight. hCMOS sensors are transformative because they provide multi-frame direct detection of x-rays at nanosecond frame-rates from the same active area (pixel) in a technology that can be customized for the x-ray energy. Existing sensors have good sensitivity for x-rays with a photon energy up to ~10 keV and new technology development is planned for capability up to ~50 keV.

The hCMOS and SLOS technologies are establishing themselves as critical tools for the NNSA stockpile stewardship program across nearly all the science campaigns and ICF. For thermonuclear burn experiments, SLOS technology enables time-resolved 3D imaging with sufficient spatial resolution to diagnose failure modes of high convergence implosions. In opacity experiments, hCMOS sensors enable time-resolved measurements of the plasma evolution essential for addressing systematic differences between models and data. In strength and phase experiments of high-pressure plutonium, hCMOS sensors will enable time-sequence measurements on a single shot (instead of using multiple shots to map out the evolution), which improves the accuracy through elimination of shot-to-shot variability and reduces the overall use of Pu on the facilities. In hostile environment experiments, high-energy hCMOS sensors will enable more detailed understanding of x-ray source physics through enhanced imaging capability that will improve the fidelity of the x-ray test environment for more precise evaluation of component survivability. There are now more than 10 diagnostics using hCMOS/SLOS technology with several more in the development phase.

hCMOS sensors continue to be delivered to Z, NIF, and OMEGA in support of existing and new diagnostic development through FY23. Work with private industry for sensor hybridization, initial testing and packaging has also been increasing. In addition, the camera system delivered to the CEA in FY19 for use in the Laser Mega Joule (LMJ) facility in Bordeaux France as part of the CEA/NNSA collaboration has been taking useful hohlraum date since its commissioning. Work to provide a second system is underway. Daedalus V2 went through fabrication and has been delivered to Z and NIF users. Initial testing has verified that it meets all original design objectives. High energy detector arrays development has started with the design, fabrication and testing of discrete pixelated arrays of GaAs photo detectors at SNL that have been hybridized to Icarus ROICs and design, fabrication and testing of discrete and pixelated arrays Ge diodes at LLNL. The time resolved diffraction diagnostic FIDDLE was commissioned in FY23 utilizing 5 hCMOS sensors and a time resolved opacity diagnostic OpSpecTR utalizing 3 hCMOS sensors completed its final design review in FY23.

Future work includes continued development of hCMOS applications around the 3 facilities as well as new integrated pulse dilation with hCMOS diagnostics. Routine multi-megajoule yields on the NIF have generated a renewed focus on radiation tolerant pulse dilation imaging. Additionally, the high speed gating intrinsic to the hCMOS architecture has show very promising radiation tolerance. It is for these reasons the High Yield X-ray Imager (HYXI) will be the first new x-ray imaging diagnostic designed to operate at 10MJ+ utilizing a pulse dilation system similar to DIXI and a new single frame hCMOS sensor (named Hyperion) develop with a commercial partner. Additionally, a second SLOS system with enhanced performance is being designed for the OMEGA laser facility providing a 3rd high-speed high-resolution line of sight. In parallel with these efforts, a new 4-frame hCMOS sensors ROIC was fabricated at the commercial Tower-Jazz 130 nm process.

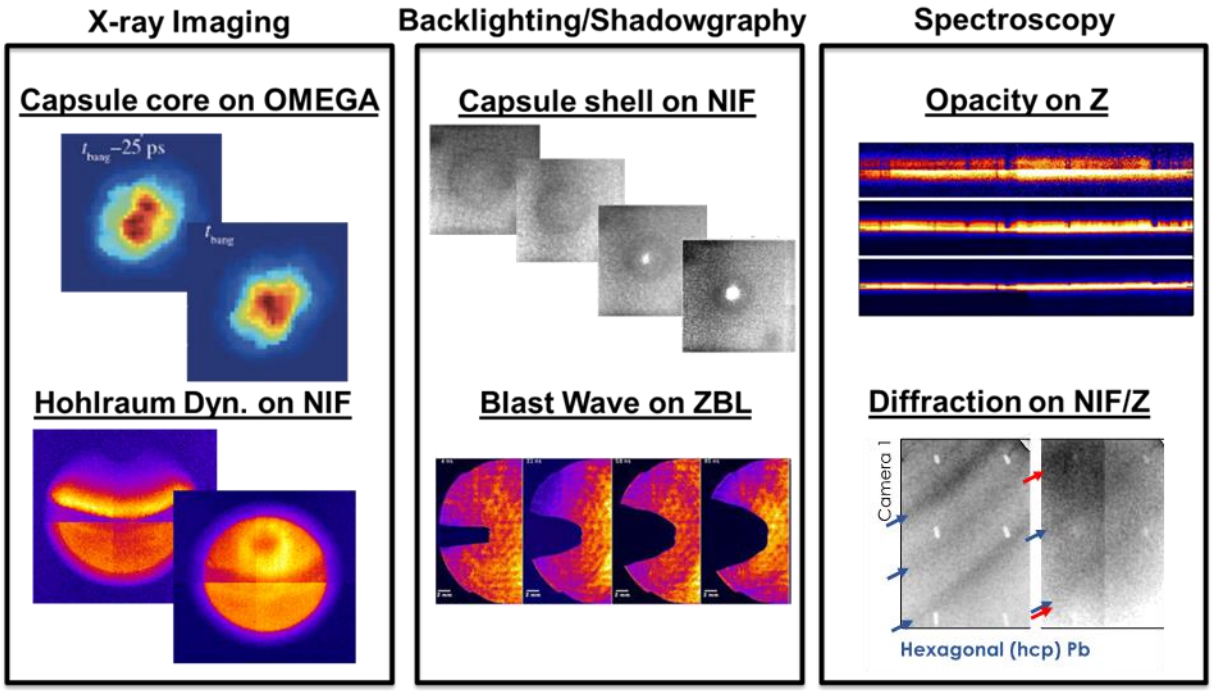

Figure 1: Example applications of SLOS- and hCMOS-enabled capabilities on NIF, Z (and the Z Beamlet Laser, ZBL) and Omega.

IIIb-2: Ultraviolet Optical Thomson Scattering (UVTS)

Optical Thomson scattering measures the spectrum of the light scattered from a mono-chromatic probe beam by a plasma, to make temporally and spatially resolved measurements of the key parameters of plasmas such as temperature, density, and flow velocity. It is the gold standard measurement for plasma properties used in tokomaks and at lower densities in ICF.

On NIF, Z, and OMEGA a high-density plasma produces high pressures to drive shocks or to inhibit hohlraum wall motion for all SSP programs. There are currently no direct measurements of the parameters of these high-density plasmas. The behavior of these plasmas needs to be better understood. Measurements of the plasma environment are

critically important to better understand hohlraum behavior, and to benchmark radiation hydrodynamics codes that presently fail to predict the complex dynamics inside hohlraums. On NIF an ultra-violet probe laser beam makes Thomson Scattering a transformative diagnostic, allowing it to probe to very high density. UVTS can also be used to access plasmas parameters at higher densities for laser direct drive.

The time evolution of the hohlraum plasma density (n_e), temperature (T_e), flow velocity and turbulence levels are critical parameters for understanding the x-ray drive for all HED hohlraum applications. Likewise, in long scale length plasmas such as Laser Direct Drive (LDD) on NIF, measurements of ne, Te, and turbulence above the critical density are important for understanding the drive pressure and its uniformity. These fundamental parameters will be uniquely measured, without recourse to integrated rad-hydro models, using Ultraviolet Thomson Scattering (UVTS) on the NIF. These parameters need to be measured at high densities (n_e is calculated to be $> 10^{21}$ e/cc in a NIF hohlraum) and in the presence of the powerful NIF heater beams. These requirements drive the need for a vacuum ultraviolet Thomson scattering probe laser beam, in order to avoid significant absorption and refraction in the plasma and so that the signal is not swamped by scattering of the 351 nm NIF drive beams. Background plasma emission and other sources of non-Thomson scattered light indicate that to exceed a signal-to-noise of unity the Thomson scattering probe laser must be 1-10J in 1ns at 210 nm, see J. S. Ross et al., Rev. of Sci. Instrumen. **87**, 11E510 (2016).

There are also many less challenging experimental configurations which can benefit from 3ω UVTS on the NIF and are benefitting from 4ω UVTS on OMEGA [for example see J. Katz et al., Rev. Sci. Instrumen. **83**, 10E349 (2012)]. These include source development for radiation effects experiments, experiments designed to study energy transport in foams, and collision-less shocks in counter-streaming plasmas. OTS has been implemented on Nova, Trident, JLF and OMEGA although in less stressing conditions than an ignition hohlraum and LDD on NIF. UVTS on the NIF is therefore a transformative diagnostic because the short wavelength of the probe opens new windows in plasma density even after five decades of Thomson scattering from high-temperature plasmas.

The detector for UVTS is a dual spectrometer multiplexing onto an ultraviolet sensitive streak camera. The detector was designed and built in FY16 [P Datte et al., (IFSA 2015) IOP Publishing], and is shown in Fig 2. It has already been used for a range of successful 3ω OTS measurements on the NIF, measuring the parameters of relatively low-density plasma for planar laser plasma instability experiments, Magnetized Liner Inertial Fusion (MagLIF) experiments, and discovery science laboratory astrophysics experiments. Data

collected by the NIF UVTS detector during Discovery science experiments investigating the formation of collisionless shocks has recently been published in Nature Physics (volume 16, pages 916–920 (2020)). More recently it has been used to make background measurements in ICF hohlraums. Initial issues with signal transmission below 180 nm have recently been resolved. These issues were tracked down to contamination of a gas volume in the streak camera. An actively pumped gas scrubbing system has been designed and installed and successfully tested. Improvements to the spectrometer housing have lead to continuous improvements in the background rejection, and changes in the mode of operation have allowed us to make the first successful simultaneous measurements of the IAW and EPW spectra on the NIF in FY22.

Figure 2: OTS detector for a DIM on the NIF.

For experiments probing ICF hohlraums on the NIF the required ultraviolet probe beam is generated by 5th harmonic conversion of a 1.05 μm glass laser beam. This is powered by an additional 10 J class laser beam line and 5th harmonic final optics assembly have been installed on the NIF to provide the required probe wavelength and energy. Commissioning experiments have begun to demonstrate the first 5ω Thomson scattering measurement. Issues with probe-to-detector co-alignment have been resolved over FY23, but no 5ω scattered signal has yet been observed. Additional testing of the system is planned in early FY24 to resolve the few remaining unknowns in the system. Assuming these tests are successful we anticipate a first 5ω signal in the first half of FY24

IIIb-3: 3D Neutron Imaging System

Three-dimensional (3D) imaging of thermonuclear (TN) burn provides the location, size, and shape of the burning region, and informs the burn and boost program of changes needed, such as improved drive symmetry or reductions in effects of engineering features such as fill tubes and tents. Gamma imaging indicates the location of the ablator material and potentially where it has mixed into the fuel, providing data that can be used to validate mix modelling.

The objective of the Neutron Imaging System (NIS) is to fully characterize the 3D fuel assembly at stagnation by imaging the neutron (primary and scattered), x-ray, and gamma-ray emission from the implosions along three almost orthogonal lines-of-sight on NIF and eventually OMEGA and Z. Three-dimensional reconstruction of non-symmetric implosions requires imaging along at least three lines-of-sight (LOS). Each LOS has two components: a pinhole aperture array that is used to form the neutron, x-ray, and gamma images (passive system), and a detector system that is used to record the image formed by

the pinhole array (active system). A scintillator-based detector with time-gated cameras on the two existing equatorial lines-of-sight allow the collection of two independently timed images from each LOS. Typically, one detector is gated to view the 14 MeV neutrons (primary image) and provides information on the size and shape of the fusion burn region. The second detector is gated at a later time to measure the source distribution neutrons which scatter off the dense fuel (scattered image), to provide information on the distribution of the cold fuel. These down-scattered neutrons are lower-energy (typically in the 6-12 MeV range) and lower-intensity and arrive after the 14 MeV neutrons. A third image can be obtained early in time to capture the 4.44-MeV gamma rays that are produced from the inelastic scattering of the 14 MeV neutrons on the ablator material through the $^{12}C(n,n\gamma)$ reaction. And now with ignition achieve and neutron yields reaching over 1E18 a fourth camera on both equatorial lines of sight will soon capture the first upscattered (reaction-in-flight) neutrons that are sensitive to mix in the cold fuel.

Computational techniques have been developed to use neutron and gamma images from multiple lines-of-sight to generate three-dimensional reconstructions of the burn region, the fuel, and the remaining ablator (Fig. 3). These advancements of the imaging system provide a measure of the 3D structure of the hot spot and cold fuel. Implementation of gamma imaging will allow measurement of remaining ablator distributions. The collection of this data enables the study of the effect of 3D asymmetry on the stagnation phase physics, and guides the development and validation of 3D models and simulations.

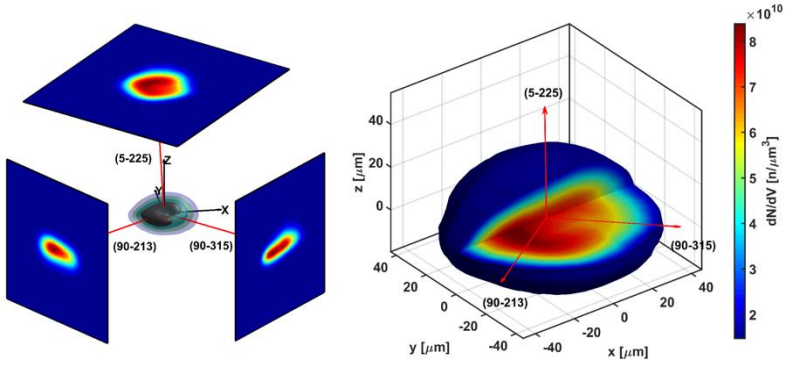

Figure 3: Neutron images from three lines of sight can be utilized to create three-dimensional reconstructions of the neutron source region and the distribution of fuel in the implosion.

Neutron imaging systems have been installed on two equatorial and one polar LOS on NIF. Currently, the polar LOS utilizes image plate as a detector and therefore the images are dominated by the greater number of unscattered neutrons. This data now allows higher quality 3D reconstructions of the primary neutron emission at stagnation.

An active system has been implemented on the second equatorial LOS approximately normal to the other two. This third system (NIS-3) includes improved active detector systems that will provide better data, and improved PinHole Array (PHA) characterization allows higher spatial resolution in the reconstructions. In addition, NIS-3 includes capability to record gamma-ray images. The gamma-ray capability was implemented in FY 2021.

Following completion of NIS-3, the improvements developed in both the passive and un-scattered and scattered neutron imaging as well as gamma imaging active systems have been applied to the original NIS-1 LOS, which was an L2 milestone in FY22. With these upgrades, NIS now provides two equatorial LOS with un-scattered and scattered neutron imaging as well as gamma imaging. The next step is to develop a gated active system on the polar LOS (NIS-2) providing three-axis views for neutrons and gammas. Current facility limitations are challenging the design and implementation of the polar LOS active system. In FY23 and FY24 there will be a series of requirement and design reviews to choose the best path forward for neutron imaging and the NIF facility. Testing of advanced cameras and scintillators is also underway in preparation for polar neutron and gamma imaging.

Neutron imaging technology developed on NIF is now being used to develop a Phase A high-resolution neutron imaging system on Z. The phase A PHA will be completed in FY24 by LANL and delivered to the Z facility with first experiments expected early in FY25.

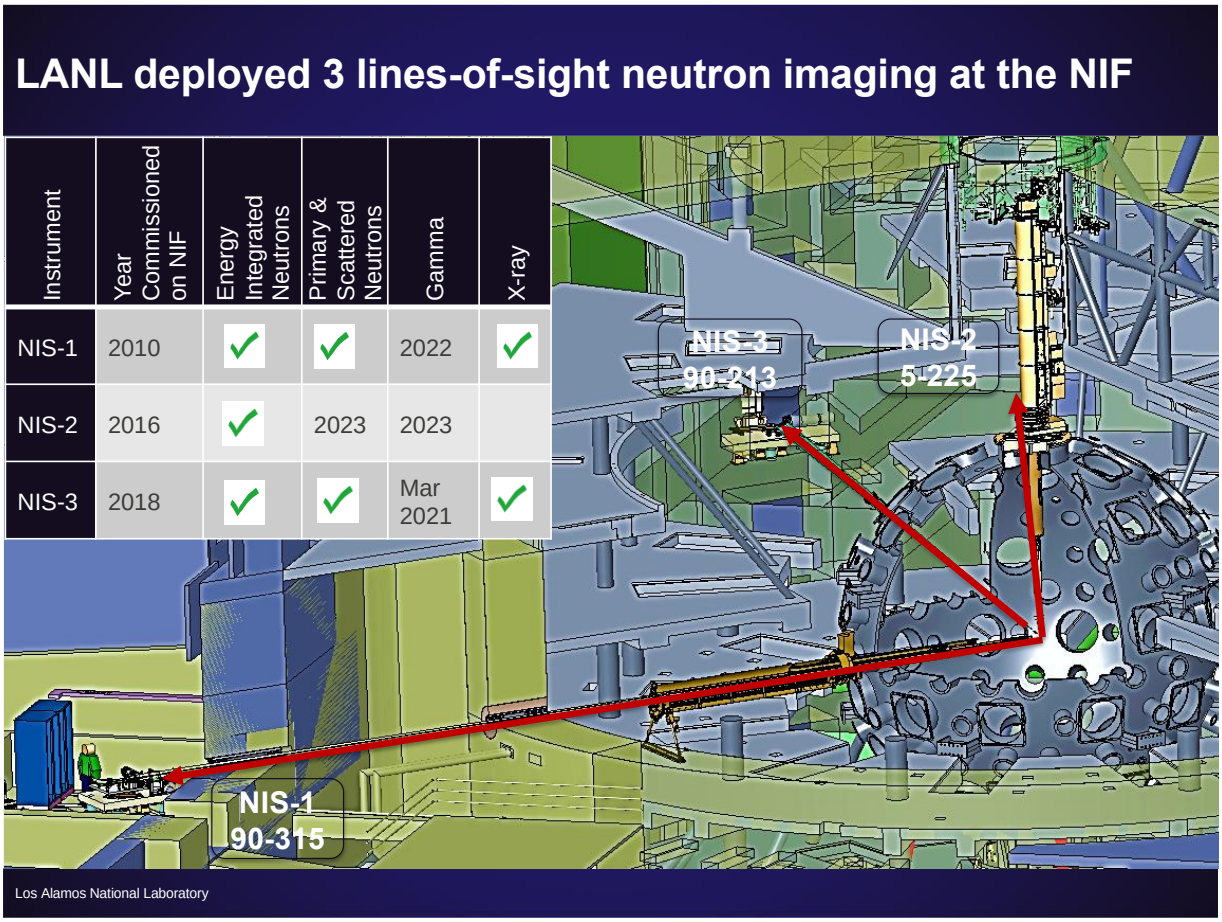

Figure 4: The Neutron Imaging System on NIF with current capabilities of each LOS identified in the table, as well as the planned dates for the incorporation of new capabilities on each LOS.

IIIb-4: Gamma Spectroscopy (GCD)

As thermonuclear burn conditions at NIF now routinely reaching an alpha-deposition regime, high-bandwidth fusion burn measurements are required beyond nuclear bang time and burn width. Since the inception of National Ignition Campaign, the Gamma Reaction History (GRH-6m) diagnostic on NIF has been providing time-resolved measurements of gamma-rays from implosions. However, GRH-6m is limited in temporal resolution by ~ 100 ps due to the technology bottle-neck of conventional photo-multiplier tubes (PMT). The objective of NIF Gas Cherenkov Detector (GCD) is to overcome these limitations in order to positively identify signs of alpha heating and/or performance degradation mechanisms such as mix and asymmetry. The GCD is also a testbed for future burn history advancements.

The NIF GCD is being developed to improve temporal resolution down to 10 ps by incorporating Pulse Dilation (PD) Photo-Multiplier Tube (PMT) technology. The LANL ICF program has been directing the development of this revolutionary PD-PMT technology, collaborating with Kentech Technologies LTD, Photek LTD, Sydor Instruments, LLNL, AWE, and General Atomics. Before coupling the PD-PMT on the NIF GCD, a double short pulse laser calibration test was performed at AWE Orion facility. Figure 5 shows the raw data from a double pulse with 135 ps peak-to-peak spacing. The blue "Undilated" trace is taken with the PD-PMT operated in dc mode as a standard PMT and results in the double pulse just barely being resolved. The red "Dilated" trace is a measurement of the same double pulse during the dilation ramp. The dilated signal is recompressed (~20x in time) to match the undilated peak spacing resulting in a highly resolved double peak structure. The resolution of the PD-PMT was found by reducing the spacing between double laser pulses and determined to be slightly less than 10 ps.

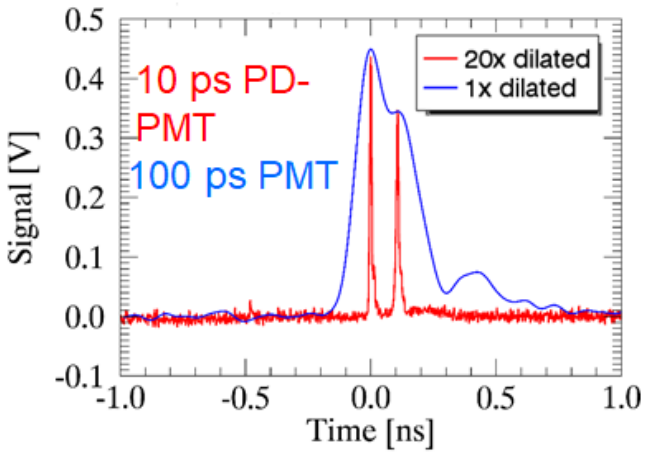

Figure 5: Two optical pulses separated by 135 picoseconds clearly resolved by PD-PMT (red curve). Standard PMT (blue curve) is just barely resolvable the two optical pulses

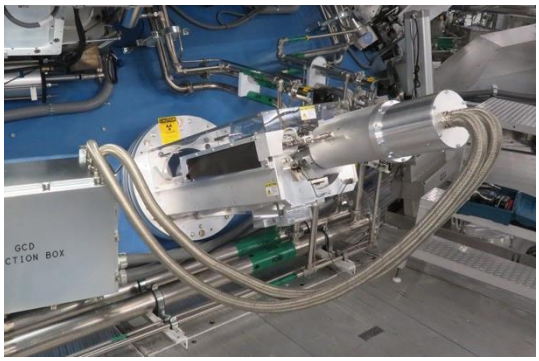

Figure 6: The NIF-GCD in the 3.9 m Well-DIM.

In late FY 2018, the PD-PMT was installed into the back end of the GCD on NIF Well DIM, completing the Installation Qualification (IQ). Shortly after, a 10x temporal magnification of carbon ablator history and DT fusion reaction history were achieved, which satisfied a NNSA L2 milestone goal (Dec 2018).

GCD took data on 35 high yield shots, 15 of those are high band width reaction histories, 20 are benchmarking and calibration shots. High band width fusion gamma reaction histories measured by NIF GCD confirm earlier fusion burn widths measured by the sister instrument GRH-6m as seen in figure 7. GCD also measured the shortest burn width ever observed at NIF on the 1.3 MJ N210808 shot of 88 ps demonstrating the benefit of its high temporal resolution. These results confirmed discrepancies between experimental data and simulations, where simulations always underpredict the burn width. This issue needs to be resolved for better understanding of inertial confinement fusion and NIF GCD can provide critical information to help resolve this problem. Additionally, the high temporal resolution of the PD-PMT will be able to resolve high frequency features such as the onset of the fusion burn that will aid in benchmarking simulations.

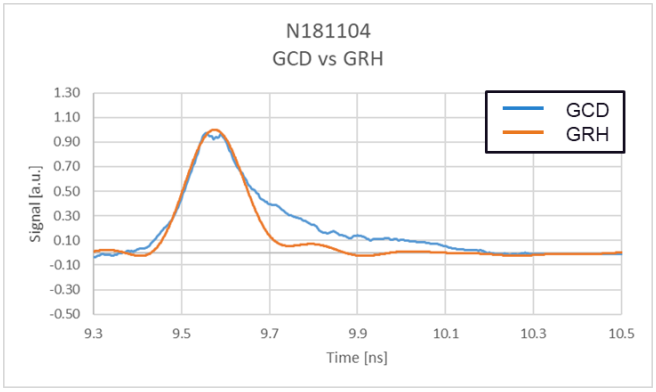

Figure 7: Comparison between High band width GCD fusion reaction history (blue) and GRH reaction history (orange).

However, the NIF-GCD fusion reaction histories showed a late-time tail component (blue curve, 9.7 ns – 10.3 ns in Figure 7), not seen in the GRH-6m. An investigation revealed that the gas cell is causing this late-time tail and not the PD-PMT itself. The current hypothesis is that gamma rays with energy below that required to produce Cherenkov radiation are causing scintillation or fluorescence in the gas cell. This signal is then collected by the GCD optics. This was not seen in the GRH, perhaps due to the circuitous optical path of the GRH, which was designed to efficiently collect the forward-directed Cherenkov radiation, but inefficiently collects the uniformly emitted fluorescence radiation.

A new NIF dedicated gas cell was installed in FY21 to uncover causes for the late-time tail. Different gases were tested and assessed for their low-fluorescence. Shielding was also added to reduce the flux of sub-threshold gamma-rays that can scatter into the gas

cell. Finally, a light block that prevents the Cherenkov radiation from reaching the PD-PMT, but allows most of the fluorescence will be added temporarily to confirm the fluorescence hypothesis. If the hypothesis is confirmed, a plan to mitigate the effect of fluorescence will be developed. One possibility is to develop a better optical path that would duplicate the ability of the GRH to efficiently collect Cherenkov radiation while rejecting fluorescence.

In addition to tests utilizing the GCD, further tests involved installing a PD-PMT on one channel of the GRH, which was completed in early FY23 and has allowed direct comparison of high-temporal resolution GRH and GCD signals. The GRH PD-PMT was fielded on several near-ignition shots and compared with GCD in FY23. These tests essentially confirmed the GRH PD-PMT removed or substantially reduced the tail signal seen on GCD, however additional measurements and characterizations of the dilation window are needed to explain some unexpectedly long burn widths.

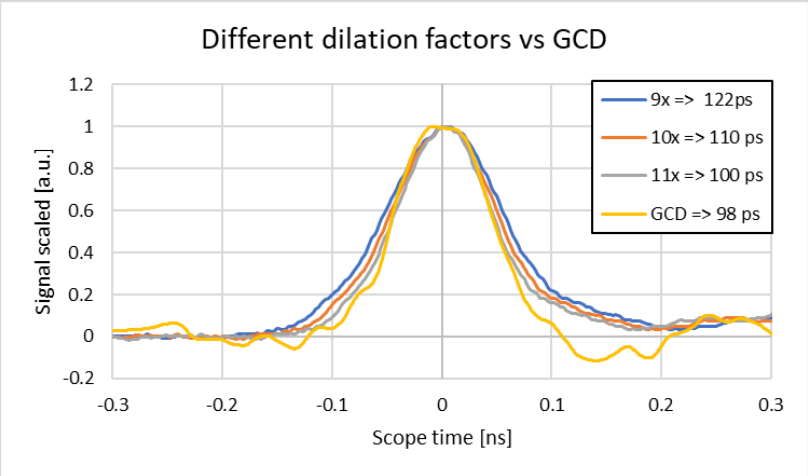

Figure 8: Comparison of the recompressed and background corrected dilated GRH fusion reaction history measurement for three different dilation factors i.e. 9x, 10x, and 11x in blue, orange, and gray respectively. The results are compared to the fusion reaction history measured by the sister instrument GCD PD-PMT in yellow

Experience from improved NIF GCD and GRH PD-PMT operations will be fed into the final phase of a NIF-specific "High-sensitivity GRH-15m" which can better handle the harsh radiation environment associated with indirect-drive and will increase dynamic-range by a few orders-of-magnitude. The resulting better data quality of high bandwidth fusion reaction histories will give a better understanding of the assembly of the hot spot, onset of the fusion burn, and truncation of the fusion burn due to developing failure modes for experiments where the neutron yield is varying widely shot-to-shot. The existing GRH diagnostic was designed to operate below 1 MJ to give optimum performance on the path to ignition. Implementing the PD-PMT on GRH has extended the operating yield limit, but at the 3-4 MJ yield range we are again approaching its

operational limit. The GRH-15m is a necessity for extending reaction history measurements in the 10 MJ range.

IIIb-5: Time resolved neutron spectrum

The transformational expected impact of time-resolved neutron spectrometry was reconfirmed in a dedicated breakout session during the Dec 2022 annual NDWG workshop, with the following motivation:

Measurements and inferences of time resolved neutron spectra have the potential to greatly impact the understanding of ICF implosions at and around stagnation, particularly in the burn-propagation regime. A long-term goal of the ICF program going forward is to increase gain (G>>1) and to understand the limits of gain at the NIF. To do this, it is important to understand why a high-gain implosion (Y1D>>1e18) 'fails,' even if it performs relatively well compared to current records. Gain is limited by a competition with pdV expansion losses, enhanced conduction, and/or ablator mix-induced radiation losses. These degradations can also prevent an implosion from reaching ignition, and the importance and impact of each degradation may change between G<<1 and G>1 because of their dependence on temperature. Time resolved DSR, apparent Tion, vHS, and yield are powerful and direct constraints on implosion power-balance during burn propagation, and also provide insights on conditions at minimum volume (potentially reducing the need for alpha-off surrogate implosions). For example, Tion(t) is sensitive to the instantaneous power balance, and DSR(t) is directly related to pdV heating and losses. Therefore, these time resolved quantities measured with sufficient dynamic range and time-resolution could help untangle low-mode, conduction, and mix failure mechanisms in implosions that fail to reach G>>1.

Historically, the primary technique pursued for making this measurement has been time-resolved Magnetic Recoil neutron Spectrometry (MRSt). The MRSt as originally proposed uses the existing MRS principle with Pulse-Dilation-Drift-Tube (PDDT) technique instead of CR-39 as the detector [J.A. Frenje et al., RSI (2016); T.J. Hilsabeck et al., RSI (2016)].

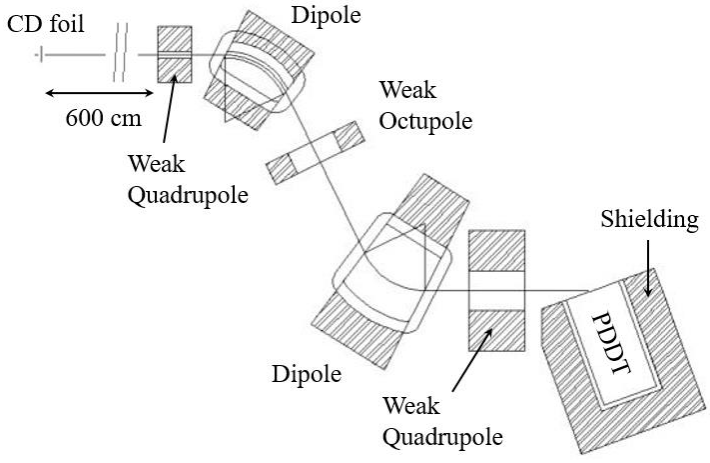

Figure 9. Main components of the MRSt design. Only the Pulse-Dilation-Drift Tube (PDDT) detector will be surrounded by shielding to reduce neutron and gamma background. The quadrupoles and octupole will be used to correct for focusing aberrations, and improve the ion-optical resolution to an unprecedented level of ~1.8 keV (100× better than current, time-integrating MRS).

The conceptual design involves a CD foil [with a thickness in the range of 25-80 μm and diameter in the range of 0.1-0.3 mm] positioned on the outside of the hohlraum for

production of recoil deuterons from incident neutrons; a system of electromagnets (**Figure 9**), positioned outside the NIF target chamber, for energy analysis and focusing of forward-scattered recoil deuterons onto a focal plane of the spectrometer; and a PDDT with a CsI cathode positioned at the focal plane of the spectrometer. In the CsI photocathode, recoil deuterons are converted into secondary electrons, which are subsequently accelerated by a spatially- and time-varying electric field that unskews and dilates the signal along the length of the PDDT. This signal is then amplified by a set of microchannel plates and then detected by an anode array. The designs of the MRSt ion-optics [G.P.A. Berg et al., RSI (2022)] and shielding [A. Sandberg, M.Sc. Thesis, MIT (2019)] are complete. The offline tests of the CsI photocathode response to ions are complete; the foil-on-hohlraum concept has been demonstrated using NIF shots [C. Parker et al., RSI (2019)]; and tests of the borosilicate MCP to background are complete [C. Parker et al., RSI (2019)]. The top-level physics requirements for the MRSt have also been defined [J. Kunimune et al., RSI (2021 and 2022)], and recent work has shown that MRSt would be expected to provide the desired measurements for implosions in the now-relevant 3-10 MJ yield range (**Figure 10**). In addition, discussions with two magnet manufacturers (Danfysik and SigmaPhi) during FY23 have demonstrated feasibility of building the magnets as designed and resulted in firm cost estimates and timelines for magnet system implementation.

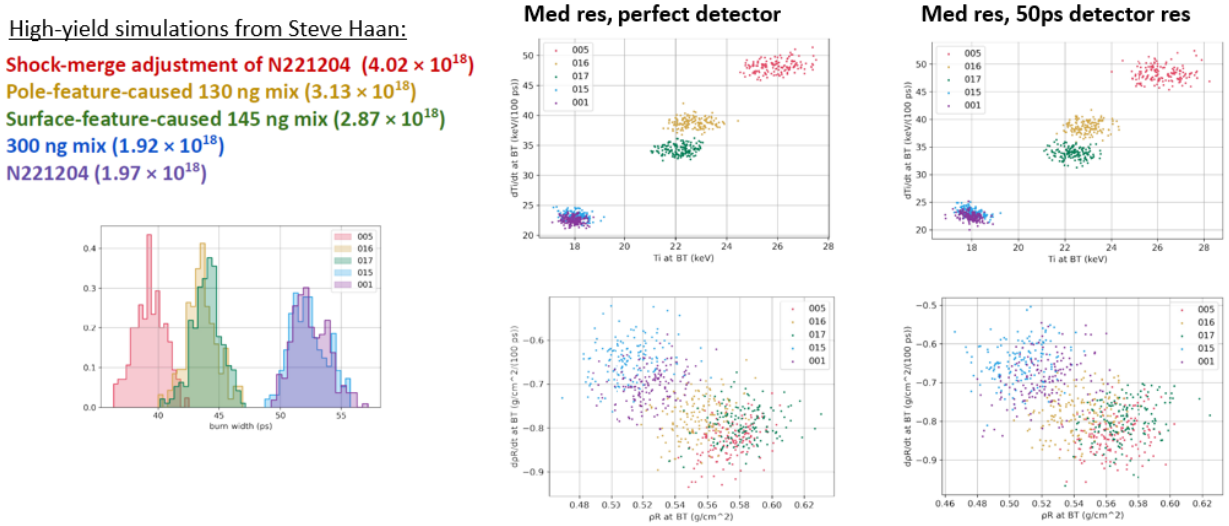

Figure 10. A synthetic data study was undertaken to evaluate MRSt performance at yields in the 3-10 MJ range, using simulated neutron spectra from high-yield rad-hydro simulations. Results suggest that MRSt would perform as desired in medium resolution mode (CD foil thickness 45μm, radius 0.25mm) both with a perfect backend detector and with a backend detector with 50 ps time resolution.

All the progress notwithstanding, there is substantial uncertainty in the feasibility of the PDDT backend detector concept, with limited progress made to date in validating this design. For this reason, it was decided during FY23 that:

- Pausing the magnet development/procurement is prudent based on the challenges with developing the detector system.
- Investigating multiple techniques for measuring time resolved neutron spectra is prudent given the challenges and costs associated with MRS(t).

- Deploying a prototype system on Omega before deployment on NIF is recommended.

An alternative method for diagnosing time-resolved neutron spectra uses multiple time-of-flight detectors along a single line of sight but located at difference distances from the source. The underlying technique can be mathematically expressed as a tomographic inversion technique, and in so doing leverages the extensive previous work on tomographic imaging in the medical and scientific fields. This technique was recently demonstrated for neutron spectra produced by a Dense Plasma Focus (DPF) device, see Figure 11. The time, flux levels, and spectral details on the DPF are quite different than on an ignited plasma at the NIF. Work must be done to: (1) verify that the analysis principle will work for expected signal, noise, and detector resolutions at the NIF; (2) conduct a proof-of-principle experiment using a near-source detector (~cm range) ideally along a common line-of-sight with another nToF detector; and (3) pursue the design review, prototyping and deployment process for diagnostics on the NIF.

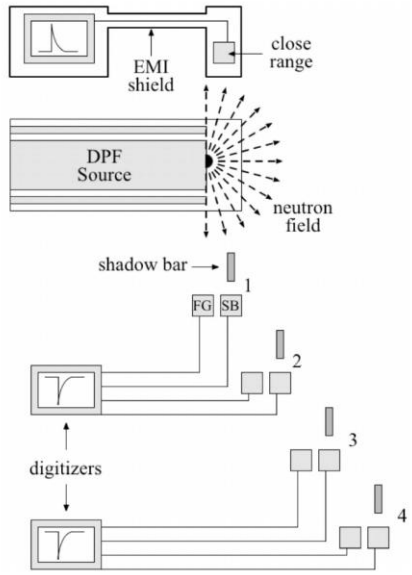

Fig. 3. Diagram of the experimental setup. The close-range detector is placed 25 cm from the pinch in the radial direction and the four shadow bar systems, comprising two neutron/photon detectors each, were placed at ranges of 10, 14, 18, and 22 m in the radial direction.

Figure 11: Experimental demonstration of tomographic reconstruction of time-resolved neutron spectra on a Dense Plasma Focus device [J. Catenacci et al., IEEE Trans. Plasma Sci., 48, 9, 3135 (2020).]

Work to demonstrate the feasibility of this tomographic technique has already begun [Figure 12]. Several enterprising postdoctoral researchers at the Lawrence Livermore National Laboratory, in conjunction with an expert in computational techniques for solving inverse problems, have developed several algorithms to reconstruct time-evolving neutron spectra. This analysis is still in the preliminary stages, and would benefit from following a path pioneered by the MRSt development [Figure 10] to evaluate sensitivities to realistic implosion conditions.

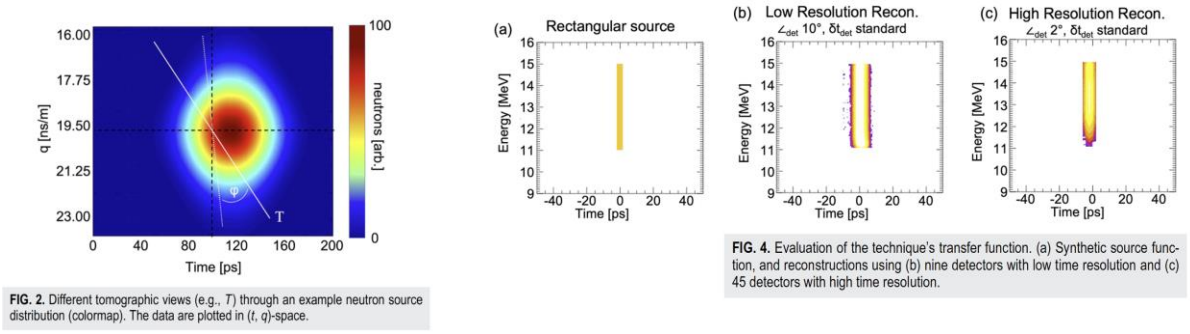

FIG. 2. Different tomographic views (e.g., T) through an example neutron source distribution (colormap). The data are plotted in (t, q)-space.

FIG. 4. Evaluation of the technique's transfer function. (a) Synthetic source function, and reconstructions using (b) nine detectors with low time resolution and (c) 45 detectors with high time resolution.

Figure 12: Preliminary investigation into the sensitivity of the tomographic reconstruction technique to obtain time-resolved neutron spectra [D.J. Schlossberg, et al., Rev. Sci. Instrum. 93, 113528 (2022).]

With the above considerations in mind, plans for FY24 include:

1. Investigating feasibility of other possible techniques for making time-resolved neutron spectrum measurements, specifically including the recently proposed "Tomographic nTOF" technique with multiple nTOF detectors fielded along the same line-of-sight at different distances from the implosion.
2. Investigating feasibility of testing backend detector concepts for the NIF MRSt with a new proposed, electro-magnet based MRS system being designed for OMEGA (MRSu).
3. Developing a simplified backend detector concept for MRSt including signal deskew capability but excluding pulse dilation.
4. Revisiting the path forward at the end of FY24 in light of new results.

In terms of milestones, this pushes a final design review to FY25, with hardware delivery in FY26 and installation at the NIF in FY27 at the earliest.

IIIb-6: High Resolution Velocimeter (HRV)

The current VISAR instrument on NIF is a highly reliable, versatile, high precision diagnostic which is run as a primary diagnostic on 100+ shots per year. However, new programmatic needs that exceed the current capabilities have emerged which motivated the inception of a new High Resolution Velocimeter (HRV) instrument including a new High-Resolution 1D VISAR, as well as a new High-Resolution 2D VISAR capability together with a visible streaked pyrometry system.

The current NIF Velocimetry Velocity (Doppler) Interferometer System for Any Reflector (VISAR) can track the velocity of a moving reflecting surface with sub % precision using a visible Laser probe at 660 nm and an interferometer to transform Doppler shift into a fringe phase shift proportional to the velocity of the reflector. A time-delay element (etalon) determines the velocity sensitivity. Specifically, the NIF VISAR is a line-imaging (1D) instrument: a f/3 optical-relay images the target onto the entrance slit of a streak camera fitted with a CCD detector. The system therefore records the velocity time-history for ~100 resolution elements corresponding to

different spatial positions onto the target. Two field-of-view options are available: 1mm and 2 mm. The spatial resolution is currently limited by the streak cameras. Space-time distortion inherent to streak-tube technology are also strongly limiting the performance, in particular around the periphery of the field of view.
The time-resolution is currently around 30 ps over a 30 ns streak.

The ICF program needs to accurately track the relative timing and speed of the multiple shock waves launched into ICF capsules (shock timing experiments) to benchmark radiation-hydrodynamic simulations of high-yield DT implosions. There is also a need to understand capsule and shock-front non-uniformities which degrade implosion quality as even very small velocity variations can seed major degradation in the implosion quality. There is therefore a need to document the velocity distribution *in-flight*, with micrometer spatial resolution and meter-per-second velocity sensitivity.

HED Stockpile Stewardship Science programs perform critical experiments to study the Equation of State (EOS), strength and phase transitions of High-Z materials using the RampEOS, RMStrength and Tardis Platforms which all use VISAR as a primary diagnostic. There is a need for sub-% accuracy in velocity, ps timing accuracy and high-fidelity imaging and recording that exceed the current capabilities. Higher spatial, timing and velocity resolution 1D VISAR would boost the data return per shot, reduce the number or NIF shots necessary to obtain the required accuracy in the EOS data (which currently requires averaging data from 3-5 shots) and would also enable new science.

Based on the programmatic needs and discussions with the users' community the new NIF High Resolution Velocimeter (HRV) instrument will have several channels to allow simultaneous recording of 1D and 2D VISARs plus Streaked Optical Pyrometry data and room to grow not to preclude future improvements. The new High-Resolution 2D-VISAR will feature f/2 and f/3 collection systems, a picosecond laser, two interferometers and 4-records per snapshot on a CCD detector. The new High-Resolution 1D VISAR will feature 4 interferometer channels for higher resolution and higher dynamic range, data redundancy and increased flexibility. A new push-pull detection scheme for higher velocity and spatial resolutions will be tested on one channel initially, before being extended to all channels. Two nanosecond lasers (blue, red) will allow us to obtain a two-color system for improved optical properties measurements. The improved Streaked Optical Pyrometry (SOP) will feature optimized stray light rejection and a detector gating to mitigate background. Overall, this combination of new and unique capabilities will make the High Resolution Velocimeter at the NIF a transformative diagnostic for the HED community.

After completing a PDR, the project was paused due to lack of available funding. The N221204 implosion with a 3 MJ neutron yield reinforced the need for enhanced neutron resilience for NIF diagnostics. The team evaluated deployment options including expanding on the existing system in the Target Bay, using the current

VISAR laser room or building a new instrument on two new floors located in the NIF switchyard. While more costly and complex to deploy initially, only the deployment in the switchyard meets the programmatic needs and neutron shielding requirements from high-yield implosions moving forward. An accelerated deployment plan was devised which calls for rapidly building three 1D VISAR channels (one channel having a Push-Pull detection scheme) with a 660 nm probe and f/3 optics while keeping the current VISAR/SOP system active.

IIIb-7: Time-Resolved X-ray Diffraction

X-ray diffraction is a well-established technique to identify phases and document phase transitions in compressed materials of interest to the SSP. X-ray diffraction is the most discriminating method to identify the phase of a solid material because it reflects the distances between atoms with high precision. The technique has been used on NIF and OMEGA, and is being developed for Z. Early work on NIF has been limited to using TARget Diffraction In-Situ (TARDIS) to obtain one or two snapshots per very expensive laser shot. Time-resolved x-ray diffraction will build on the demonstrated success of the TARDIS (NIF) and Power X-ray Diffraction Image Plates (PXRDIP, Omega) platforms to provide a significant enhancement to the HED materials diffraction program for the SSP.

The ability to observe material phase at multiple times during a solid-solid or solid-liquid phase transition within a single laser experiment will substantially constrain equilibrium material phase boundaries and also enhance our understanding of kinetic effects that drive or inhibit phase transformation in materials at high densities. Moreover, we anticipate that the time-gated quality of these measurements will improve the signal to noise of measurements as background signals (which are substantial) are not integrated over the entire experiment. With this platform our facilities will be able to make multiple diffraction measurements of a solid material compressed to multi-Megabar pressures over timescales as long as tens of nanoseconds.

We evaluated several approaches to a time-resolved diffraction platform. To maximize detection efficiency, we have decided on a direct-detection strategy in which an x-ray sensitive detector is placed very close to the target. This strategy ultimately will allow us to minimize the heating of the target, which is critical to document certain phase transitions and to prevent melting of solid targets. In the first years of XRD(t) development we designed and commissioned a Gated Diffraction Development Diagnostic (G3D) to confirm the feasibility of this approach. We completed fifteen NIF shots with the G3D between 2019 and 2022.

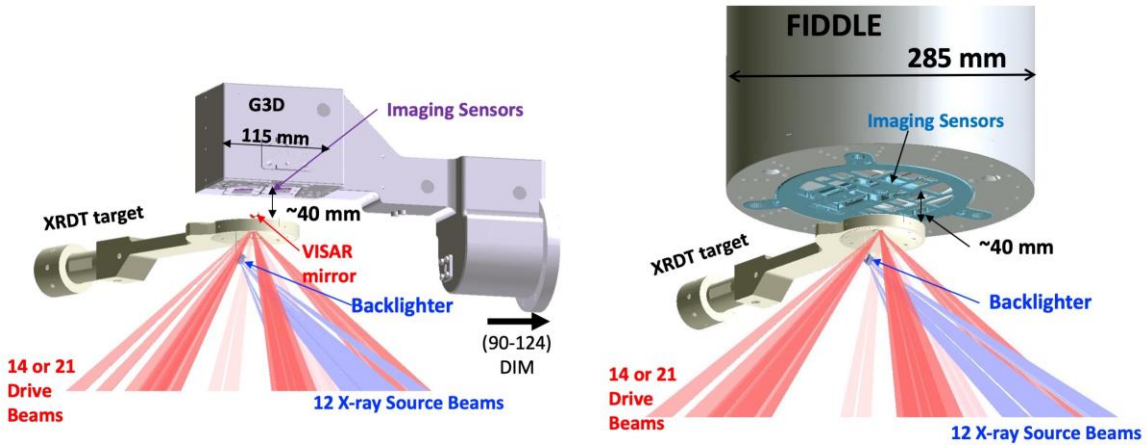

Figure 13: Time resolved x-ray diffraction platform. FIDDLE (right) uses the same XRDT target, laser drive and backlighter as the development diagnostic (left). FIDDLE has more sensor area and better calibration to produce quantitatively better diffraction data.

Status update, 2023 (NIF)

Having successfully demonstrated that direct detection is feasible, we are now turning our attention to the design and build of a robust experimental platform that will be able to make high-quality diffraction measurements for a wide variety of material transformations. The Flexible Imaging Diffraction Diagnostic for Laser Experiments (FIDDLE) was built and fielded on NIF in 2023.

Final Design Review for FIDDLE-A was conducted in November 2022. This first iteration of the FIDDLE diagnostic is comprised of five Icarus sensors, due to delays in delivery of the faster Daedalus sensors. The next iteration of the diagnostic (FIDDLE-B) is expected to include eight Daedalus sensors as well as a streak camera to identify transitions that may be faster than the ns scale of the imaging sensors. FIDDLE-B is expected to be commissioned in FY25.

Diagnostic build proceeded in stages as calibration activities were performed on several subassemblies before they were integrated into the full FIDDLE. Before integration into FIDDLE the sensors were calibrated individually for functionality and response to off-gate incident light. After integration with all necessary cabling, the sensors were also co-timed to each other. Sensor locations were calibrated relative to the center of the FIDDLE barrel using a coordinate-measurement-machine (CMM) after they were installed into the FIDDLE front end. Finally, after the air-barrel was assembled (see figure 14), locations of the ATLAS retroreflectors were calibrated at the snout characterization station in the Target Diagnostics Factory to ensure that the diagnostic alignment plan could proceed successfully.

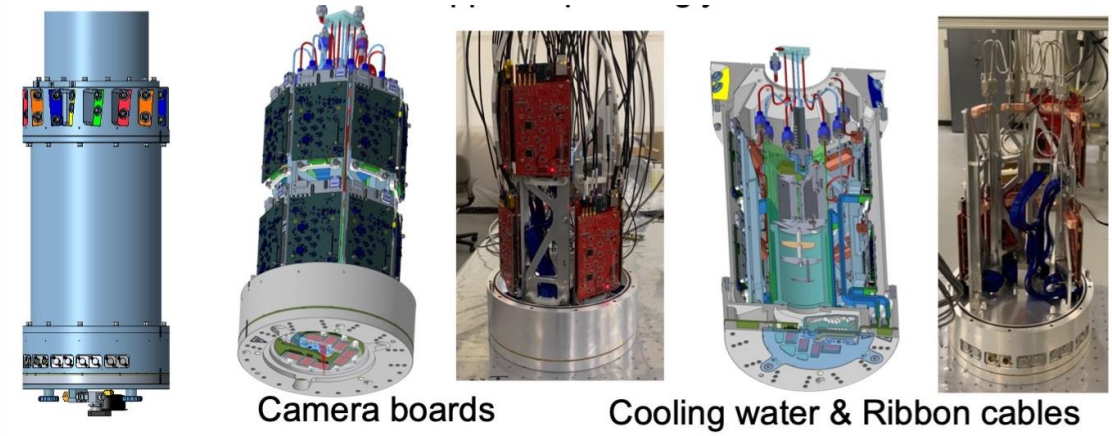

Figure 14. FIDDLE barrel during assembly compared to images from CAD model. ATLAS retroreflector locations along the top and bottom of the barrel were calibrated to ensure smooth alignment during shot operations.

FIDDLE was fielded on a NIF shot in July 2023 (N230727-001). Although the detectors were overwhelmed with background signal on this first shot, we have since then identified several additional shielding elements shot that we expect will substantially improve the diffraction signal on our next shot, scheduled for September 28, 2023.

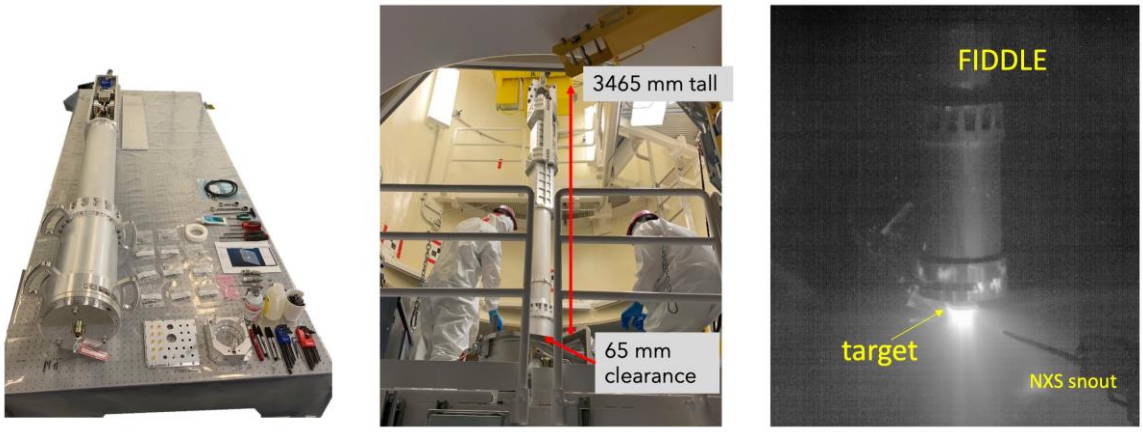

Figure 15: New FIDDLE diagnostic: (left) during assembly; (center) during installation above the polar DIM; (right) during NIF shot N230727-001-999.

Status update, 2023 (Omega-EP)

During this reporting period we succeeded in measuring time-resolved x-ray diffraction at the Omega-EP laser. After several experimental configurations that produced unacceptable levels of background, we found that an x-ray framing camera integrated with a PXRDIP target provided the most-effective shielding.

With this experimental configuration we were able to begin assessing signal quality and linewidth of an Fe target before, during, and after shock compression. We anticipate that the high temporal resolution of the x-ray framing camera (as fast as

100-200 ps) will help distinguish the Omega XRDT platform from the NIF platform, but we still need to work to understand the quality of the data and the accuracy of diffraction intensity. Our next shot day is scheduled in October 2023.

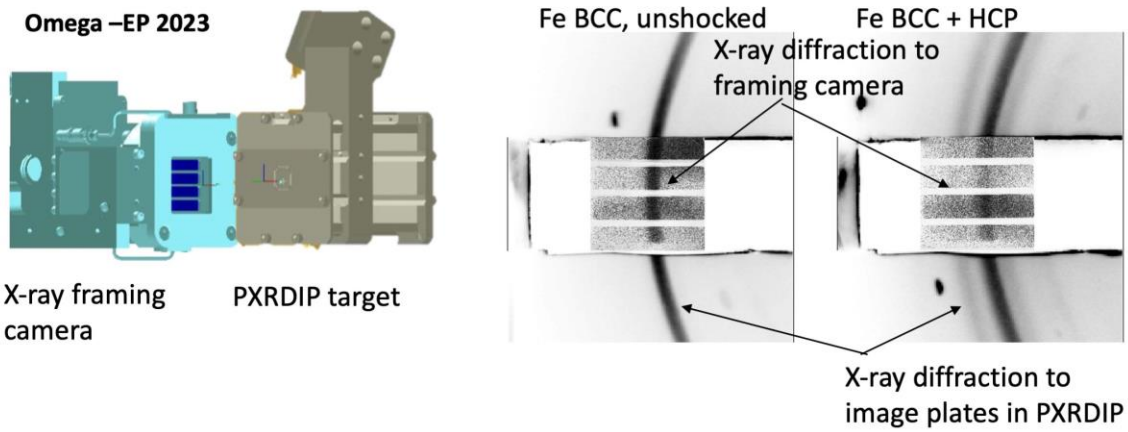

Figure 16: Time-resolved x-ray diffraction at Omega-EP. (left) Experimental platform in 2023 used an x-ray framing camera next to the PXRDIP. (right) X-ray diffraction from uncompressed and shock compressed iron targets.

IIIb-8: >15 keV X-ray Detection (DHEX)

There is currently a gap in the ability to efficiently **d**etect **h**igh **e**nergy **X**-rays (DHEX) with multi-frame capability across many HED applications and programs. This ability is becoming increasingly important, in particular as experimental investigations move to probe plasmas of higher density and temperature, or larger volume, which needs higher X-ray energies and therefore efficient HE X-ray detection.

As the U.S. are developing X-ray sources to study plasmas of higher density and temperature, or larger volume, at high repetition rates, it is our responsibility to also develop the detectors for these applications. There is currently a gap in the ability to efficiently detect high energy X-rays with multi-frame capability. With new technologies and advances in other fields, we can potentially close and fill the need of advancing and developing high energy X-ray detection for multiple applications. The initiative would extend beyond the current available detector capabilities worldwide and keep the U.S. at the forefront of scientific progress pertinent to high-density regimes that are relevant to stockpile stewardship.

Goals:

- Efficient x-ray detection at high energies (>15keV)
- GHz, Multiple frames & high data rate, fast detection

Developing higher energy X-ray detectors with multi-frame capability is important for several HED facilities around the world. Such a capability would allow observation of the evolution of a single driven target down to the sub-ns timescale, which would increase the quality of data both by combining what would be a multi-shot sequence into one and

by removing uncertainties arising from variations in target and laser conditions. There would be similar advantages for HED science in NNSA missions, for example time resolved diffraction for diagnosing material properties of shocked materials at high strain rates. A high Q/E detector at > 10keV with <nanosecond frame duration that could provide multiple frames would reduce the number of experiments required to map out material phase space as a function of material pressure. This would reduce both the cost of experiments and reduce uncertainties arising from comparing trends across multiple experiments.

Applications include high pressure drivers like the Omega and NIF lasers and advanced light sources that are moving to higher X-ray energies. A flexible ability to modify the data acquisition rates in 100s's ps to nanosecond ranges would open up new science at these facilities.

Ways to detect high-energy (HE) X-rays can be put into two categories, bulk (diode) and electron (photocathode) detection. These two approaches differ in temporal resolution, ns vs 10s of ps scales.

Currently available photodiode-based detectors use 25 and 50 µm thick Si diodes which only work well for ~5 keV X-rays. Moving to thicker, 100 µm - 200 µm Si diodes would increase the absorption for HE X-rays. Unfortunately, a thicker photo diode (PD) detector structure results in slower performance and blooming between pixels and though Si has a very high technology readiness level (TRL), for HE X-ray detection it requires an unfeasible thickness. This causes as slow temporal response in the 5ns to 10ns range, and the expected absorption is only about 10% at 25 keV.

Other PD materials that are currently under development such as GaAs and Ge are of lower TRL but are promising with regards to improved X-ray detection at higher energies while having a fast expected temporal response. Ongoing work at SNL includes pixelated GaAs diodes with 40 µm thickness, and expected 40% absorption @25 keV, and 0.44 ns expected temporal response. LLNL is working with UC Davis on a Ge pixelated diode with expected 50% absorption @ 25 keV for 60 µm Ge with a temporal response of 1 ns.

The diodes can be bonded to fast Read Out Integrated Circuits (ROICs) which are physically large: millions of pixels. For hard X-rays the number of electron-hole pairs generated quickly saturate the readout. Mitigation strategies are being investigated, such as larger full-well capacities and charge dumping schemes. Work to increase the full well capacity of existing ROICs has recently focused on the use of high-k dielectrics in the MIM Capacitor including HfO2 and Al2O3. This work has shown promise as a simple process step change to existing designs with no other re-tooling required to achieve up to 5x the full well. In FY22 20 µm GaAs diode arrays where integrated with the ICARUS V2 sensors, however, a packaging issue prevented the sensors from functioning. In FY23 a new batch was packaged that delivered the 1st testable GaAs hCMOS sensor. While ns-fast framing is not possible on this sensor due to a shorting issue, preliminary images and gate profiles were taken. Work is ongoing to demonstrate first fully functional

nanosecond fast GaAs imager next year and to investigate the potential of InP for even higher QE for > 30keV.

Due to budget limitations and the success of GaAs the scope of work on the Ge photodiode effort has been reduced and this trend is expected to continue into FY24. Ongoing work to develop a successful etching process has shown promise with good etch control using an electrolytic etch process that can determine the etch layer through current monitoring. Successful QE testing of individual Ge photodiodes at ALS up to 28 KeV showed results consistent with simulation and work on developing advance super-junction structures was studied in simulation.

Plasmas and material research can require temporal resolution faster than the ns scale where a photocathode approach is more appropriate. For this streak cameras and pulse dilation aided framing cameras (another transformative diagnostic) can have short integration times. The state-of-the-art X-ray detectors use photocathodes and diodes that use 'old, common' materials and suffer from degrading/poor detection efficiencies for higher X-ray energies which make detection of >10 keV X-rays challenging. An ideal PC material has a high X-ray stopping power, low electron pulse height distribution, and large escape depth for the secondaries as well as a low primary contribution. In other words, it would absorb all photons and produce only one low-energy electron per photon. However, currently available X-ray PCs usually obtain noisy images because each photon can produce a wide range, 0 to 100's, of electrons per absorbed X-ray, so has high pulse height distributions. In addition to the large electron distribution, the detection sensitivity of these PCs usually drops by an order of magnitude between 5 and 15 keV. This means that the Detective Quantum Efficiency (DQE) is < 0.5% for the X-ray energies under consideration.

A possible way to improve the Quantum Efficiency (QE) for PCs is to increase the interaction area per unit area (i.e. increase QE without changing the electron distribution or noise factor (NF)). Both, structured PCs and MCPs as PCs offer a geometric way to increase the interaction/absorption length by lengthening the X-ray path while maintaining a short escape length for the electrons. Here the transit time distribution and energy distribution of secondary electrons limits the achievable temporal resolution. Structured photocathodes have already shown a QE improvement of 3.4× with Au PC At 7.5 keV. Assuming that the NF does not change this is equivalent to an improvement of 1.8× in SNR. Even steeper structures are predicted to give a 10× boost in QE, translating to a 3× improvement of the SNR. This technique could be especially useful for detecting higher (>10 keV) photon energies. However, the temporal fidelity still needs to be studied, as well as coating methods for Alkali Halide PC materials for these structured PCs need to be established. In addition, studies into decreasing the NF, i.e. increasing the dynamic range of the PCs by reducing the number of high charge bunches using an electron beam filter are required and in some cases are underway.

For the integration of higher QE photocathodes we have decided to focus on the MCP as a PC path. A modified streak camera test apparatus is assembled to measure both the transit time spread and energy distribution of the output electrons. Unfortunately, due

delays and resource limitation, this project has been further delayed, but testing is planned for FY24.

Detecting high energy photons produces a large number of primary and secondary electrons per absorbed photons. This can lead to excess charge build up, space charge effects and reduced dynamic range of the detectors. Mitigation schemes are required for these space charge issues. As discussed above, some work is underway in this area, but more work needs to be done to characterize the issues and (hopefully) solve them. Particle-in-Cell codes are useful as a means of modeling the behavior of these instruments. More effort is required to adapt existing codes and develop new tailored models to understand these important issues.

IIIb-9: hCMOS

The hCMOS technology developed at Sandia's Microsystems Engineering Science & Applications (MESA) facility is the world's fastest, multi-frame, burst mode imaging sensor capable of capturing images on the nanosecond timescale. hCMOS sensors can detect and image X-rays, visible light, and energetic electron and have been established as a critical tool for the NNSA stockpile stewardship program across nearly all the science campaigns and ICF. For thermonuclear burn experiments, hCMOS (in conjunction with SLOS technology) enables time-resolved 3D imaging with sufficient spatial resolution to diagnose failure modes of high convergence implosions. In opacity experiments, hCMOS sensors enable time-resolved measurements of the plasma evolution essential for addressing systematic differences between models and data. In strength and phase experiments of high pressure plutonium, hCMOS sensors will enable time-sequence measurements on a single shot (instead of using multiple shots to map out the evolution), which improves the accuracy through elimination of shot-to-shot variability and reduces the overall use of Pu on the facilities. In hostile environment experiments, high-energy x-ray sensitive hCMOS sensors will enable more detailed understanding of x-ray source physics through enhanced imaging capability that will improve the fidelity of the x-ray test environment for more precise evaluation of component survivability. There are now more than 25 diagnostics using hCMOS/SLOS technology.

hCMOS technology provides three key benefits to many ICF and HED diagnostics und development; multi frame sampling from same pixel (active are), gating out of background, and native radiation tolerance. The hCMOS sensors and LLNL developed camera electronics are currently the most radiation tolerance imagers on NIF. This radiation tolerance and ability to gate out unwanted background is a growing benefit to the programs for both high yield and high background experiments.

Over the fifteen year development of hCMOS sensors at Sandia first and then part of the national program has resulted in multiple unique sensor configurations that have demonstrated their value on Z, NIF, Omega, LMJ, and other facilities. At this point, we consider it a nearly mature technology with a documented and

demonstrated process flow to both hybridize ROIC and diode wafers, and to package individual parts. There is also now a private company, Advanced hCMOS Systems (AHS), that can manage that process flow and can be contracted by any one of the labs to provide characterized sensors. The Pulsed Power Sciences Center at Sandia will therefore be phasing out of being the community provider for these sensors over the next year. Cost sharing for fabrication and sensor realization of existing mature designs such as Icarus V2 and Daedalus V2 will need to be supported by the individual project that is planning to utilize hCMOS sensors.

LLNL has contracted with AHS to develop a new radiation tolerant hCMOS single frame sensor for the High Yield X-ray Imager. This sensor named Hyperion is designed to meet the temporal, spatial resolution/area, and radiation environment requirements for use on >10MJ yield experiments on the NIF as part of the High Yield X-ray Imager (HYXI) expected in FY26. After this initial application X-ray streak cameras will be hardened and have performance improvements through the implementation of Hyperion sensors and associated radiation tolerant camera electronics.

IV: Broad Diagnostic Efforts

The NDWG defined a class of diagnostics or diagnostic related activities which benefits from significant national efforts and will enable new or more precise measurements across the complex. These are: Precision nToF, Mix, and Te, Image Analysis, Hard X-Ray Detectors, X-ray Doppler Velocimetry (XDV), and Synthetic Data. There is also an ongoing effort to maintain the capability to scan imaging plates with high accuracy and consistency across the complex.

One part of the precision nToF activity is to continue improving the measurement accuracy of the hot-spot velocity inferred from the nToF spectrum. Existing nToF detectors provided the first evidence that DT implosions at both NIF and Omega have a residual bulk velocity limiting the efficiency of the implosion. Both direct and indirect drive experiments have confirmed the adverse impact of residual hot-spot velocity on fusion yield and was confirmed with simulations.

Measuring the hot-spot velocity requires better than 10000:1 precision owing to the relatively small drift velocity ~10-100km/s that modifies the birth neutron spectrum that has a velocity associated with the 14 MeV neutron of 51233km/s. A simple hot-spot model asserts that the mean neutron energy is modified by both bulk hot-spot motion and the average kinetic energy (or ion temperature) of the D and T reactants. To characterize the 3D velocity vector and ion temperature a minimum 3 or 4 independent nToF detectors are required at quasi-orthogonal positions around the target chamber. Each of these must be sufficiently well collimated so that the neutron spectrum is not significantly impacted by the scattering environment and of sufficient temporal response to meet the precision requirements described above. This need has led to a multi-laboratory goal within the nToF community to implement more collimated lines of sight and faster fused-silica Cherenkov nToF detectors to better characterize the bulk flow. In addition adding a fifth detector on NIF has improved the accuracy of the velocity measurement as shown in

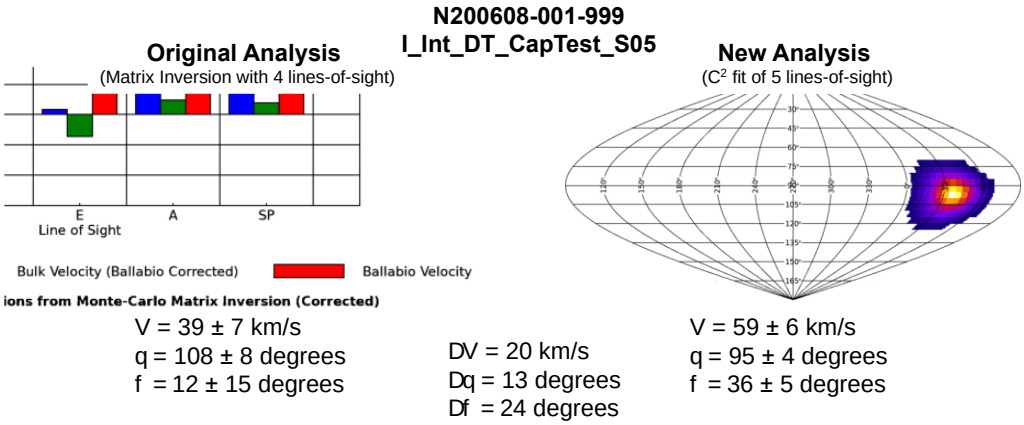

Figure 17 -Analysis of hot spot velocity using 4 NTOF LOS vs 5 LoS, which has improved both the angular precision of the velocity measurement by ~2x.

Fused-silica Cherenkov nToF detectors (QCD) have enabled higher precision velocity measurements illustrated in Figure 17 due to the thresholding nature of the Cherenkov process. This means that the signal measured due to gamma-rays is more directly related to the implosion bang-time and not polluted by high-energy x-rays emitted by LPI in the hohlraum or plasma surrounding the capsule.

This has revolutionized the precision with which hot-spot bulk flow can be measured and as a result, Cherenkov detectors have been deployed and tested at NIF, Omega and Z over the past 2 years. All 3 laboratories are investing in additional nToF lines of sight to better understand these effects which should lead to a significantly improved capability within the next few years.

NIF to Z Diagnostic Tech Transfer Effort:
After a decade of intense investment, there are well established diagnostic capabilities demonstrated at the NIF that are used to make quantitative measurements on ICF plasmas. Many of these diagnostics were developed as national collaborations toward the goal of determining the efficacy of NIF to achieve ignition. Starting in late 2020 a tech-

transfer effort was initiated to transfer key measurement capabilities and engineer for use at Z. These demonstrated capabilities on the NIF will bring the measurement maturity for characterizing magnetic direct drive (MDD) fusion plasmas on Z up to the long-standing ability of the NIF.

Nuclear burn volume, burn and confinement time, burn magnitude (and spectra), and ion burn temperature are fundamental to quantifying burn performance. At present, Z has no capabilities to measure neutron production duration (burn width), the spatial length scale for 1D neutron imaging is ~0.5 mm, and there are no capabilities to disambiguate effects of motion broadening of neutron spectra from a thermonuclear ion temperature. While substantial understanding can be gained with integrated measurements, multi-dimensional spatially and temporally resolved data is critical to assess key questions on performance and scaling and to utilize burning platforms for stockpile science. The physics requirements for spatial and temporal resolution in nuclear and x-ray measurements in some MDD platforms require existing capabilities on Z to improve by roughly an order of magnitude (detailed physics requirements available in classified document). For typical ICF plasmas, the feature length scales of interest are ~10 micrometers and ~10 picoseconds and require nuclear diagnostics to most effectively assess. On NIF, typical measurement error for scalar fusion output metrics is less than 10%, and in some cases routinely less than 5%. The technology to make each of these measurements on NIF are routine and in some cases have been deployed along multiple lines-of-sight.
The specific capabilities under development as part of this NIF-to-Z technology transfer include:

- Improved nTOF for reliable Tion and kinetic energy: During the latter stages of the National Ignition Campaign (NIC), it became clear that a significant amount of residual kinetic energy (RKE) was present during the burn phase of the implosion. This RKE manifested itself in significantly shifted and broadened neutron time-of-flight signals. Quantifying the RKE requires measuring the neutron time-of-flight (nTOF) signals along multiple independent nTOF lines of sight to fully disambiguate coherent and incoherent flow, as well as the true burn weighted ion temperature, Tion.
- X-ray streak bang and burn: Understanding stagnation conditions is greatly enhanced through an analysis based on both X-ray and nuclear signatures. One gap in the X-ray diagnostic suite at the Z-facility is the lack of X-ray streak camera-based instruments. At the NIF, X-ray streak cameras are regularly used to provide high temporal resolution X-ray burn history measurements (SPIDER), high temporal resolution 1-D images of implosions (DISC), and high temporal and spatial resolution spectroscopy measurements (DISC/tConSpec).
- 2-D neutron imaging: At Z, there is no 2-D neutron imaging capability, while there is a 1-D capability it is limited by a spatial resolution of 0.5mm. A highly resolved 2-D neutron capability will be transformational to help understand and resolve fusion parameters such as the burn volume and shape, which is critical to infer ignition metrics such as P-tau.

V: Local diagnostic development efforts at NIF, Z and OMEGA

V-1: Local Diagnostic Development on the National Ignition Facility

New local diagnostic capabilities on the NIF are aimed at improving our understanding of the evolution of high energy density plasmas for stockpile stewardship, National Security applications and discovery science. The majority of the development activities in FY 22 were focused on the development of x-ray, neutron and optical diagnostics for LLNL HED science programs, including Inertial Confinement Fusion (ICF), focused high energy density experiments, specifically: Materials research and radiation transport. For ICF these local diagnostics can be categorized into three general areas, (1) Hohlraum drive, (2) Capsule response and (3) Stagnation diagnostics.

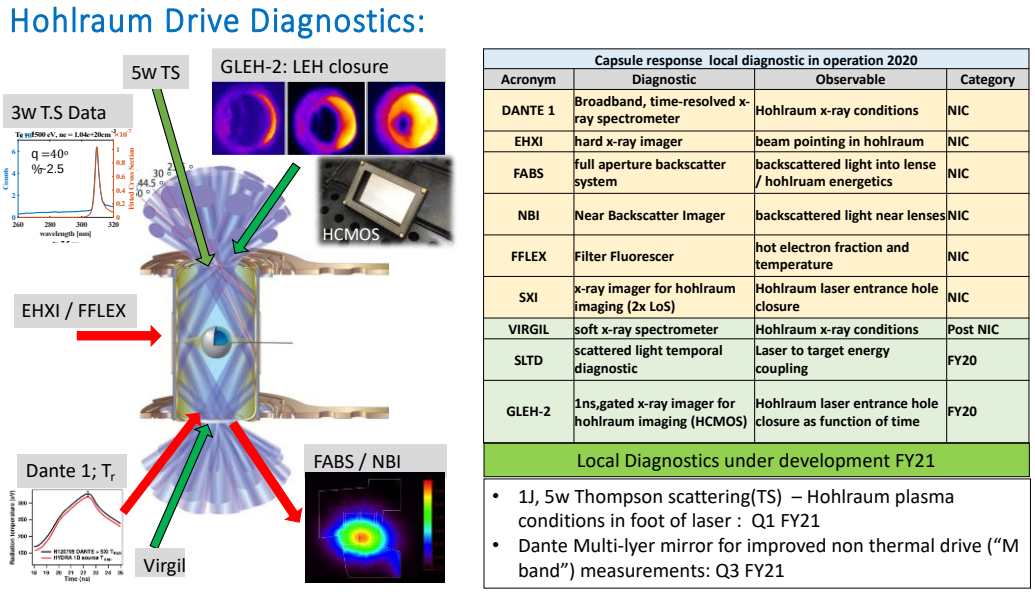

Capsule response local diagnostic in operation 2020			
Acronym	Diagnostic	Observable	Category
DANTE 1	Broadband, time-resolved x-ray spectrometer	Hohlraum x-ray conditions	NIC
EHXI	hard x-ray imager	beam pointing in hohlraum	NIC
FABS	full aperture backscatter system	backscattered light into lense / hohlruam energetics	NIC
NBI	Near Backscatter Imager	backscattered light near lenses	NIC
FFLEX	Filter Fluorescer	hot electron fraction and temperature	NIC
SXI	x-ray imager for hohlraum imaging (2x LoS)	Hohlraum laser entrance hole closure	NIC
VIRGIL	soft x-ray spectrometer	Hohlraum x-ray conditions	Post NIC
SLTD	scattered light temporal diagnostic	Laser to target energy coupling	FY20
GLEH-2	1ns,gated x-ray imager for hohlraum imaging (HCMOS)	Hohlraum laser entrance hole closure as function of time	FY20

Local Diagnostics under development FY21

- 1J, 5w Thompson scattering(TS) – Hohlraum plasma conditions in foot of laser : Q1 FY21
- Dante Multi-lyer mirror for improved non thermal drive ("M band") measurements: Q3 FY21

Figure 18: ICF Hohlraum Drive Diagnostics: *Hohlraum Drive Diagnostics, including example data from Gated Laser Entrance Hole (GLEH) imagers that utilize hCMOS technology, 3w Thomson Scattering, Radiation temperature measured by Dante 1 and backscattered light distribution measured by the NBI and FABS diagnostic. The table shows diagnostic, observables and time frames for first implementation.*

The hohlraum drive local diagnostics, shown in Fig.18, include soft x-ray spectrometers (e.g. Dante 1 and Virgil), hard x-ray spectrometers (FFLEX), hohlraum alignment imagers (EHXI and SXI) and scattered light diagnostics (SLTD, FABS, NBI). The NIF scattered light time history diagnostic (SLTD) was developed for LDD to measure the azimuthal distribution of scattered light in NIF polar direct drive implosions. Major developments in this area are a new gated laser entrance hole imager (GLEH-2), which has replaced the standard CCD camera in SXI with SNL's time gated hCMOS cameras. This now provides 1 ns duration time gated images of the hohlraum laser entrance hole (LEH) and feeds into assessments of both laser-hohlraum energy coupling and implosion symmetry. The second major development is the addition of the transformational deep UV Thomson scattering diagnostic, which is due to come online late by mid FY23 and will greatly benefit diagnosis of hohlraum and coronal plasmas for HED science. This system uses a 5ω optical probe to capture light scattered from the ion-acoustic wave in FY23. This provides time resolved

point measurements of temperature, plasma flow and plasma ionization stage in the hohlraum plasma (this system is described in detail in transformational section A.A). In FY24 we plan to add the electron-plasma wave measurement which will add a measurement of plasma density in the hohlraum.

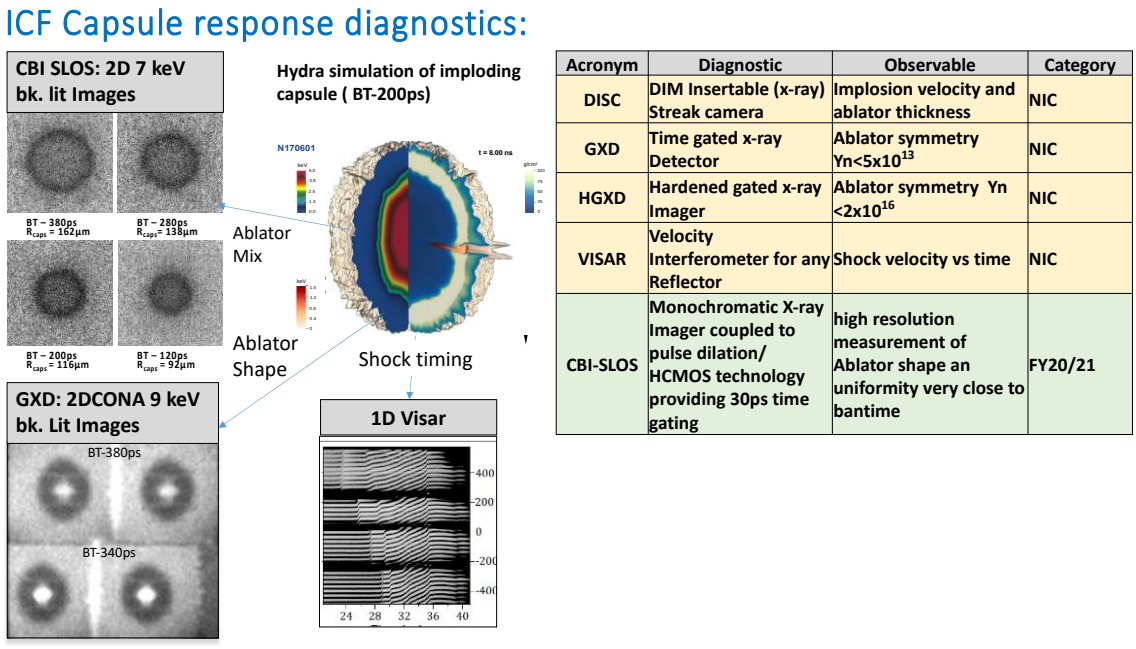

Acronym	Diagnostic	Observable	Category
DISC	DIM Insertable (x-ray) Streak camera	Implosion velocity and ablator thickness	NIC
GXD	Time gated x-ray Detector	Ablator symmetry Yn<5x10^{13}	NIC
HGXD	Hardened gated x-ray Imager	Ablator symmetry Yn <2x10^{16}	NIC
VISAR	Velocity Interferometer for any Reflector	Shock velocity vs time	NIC
CBI-SLOS	Monochromatic X-ray Imager coupled to pulse dilation/ HCMOS technology providing 30ps time gating	high resolution measurement of Ablator shape an uniformity very close to bantime	FY20/21

Figure. 19: ICF Capsule Response Diagnostics, showing a hydra simulation of a capsule within 200ps of bang time, four examples of important diagnostic measurements during NIC (1D VISAR, 2DCONA), post NIC (CBI-SLOS).

2.2. Capsule Response Local diagnostics:

For laser indirect drive the hohlraum produces a large flux of soft x-rays which are absorbed in the capsule containing the DT fuel. The outer wall of the capsule (the "ablator") is heated by the x-rays and expands rapidly, driving a series of shocks that travel through the ablator and fuel, leading to a quasi-spherical implosion that both compresses and heats the DT fuel. Capsule response diagnostics are required to measure the symmetry and performance of the ablator and fuel as it implodes.

Capsule response diagnostics are shown in Fig.19. Just after the completion of NIC, the ablator uniformity, density and symmetry were measured using backlit 2D x-ray radiography (2DCONA). This technique uses an x-ray backlighter to provide a shadow of the ablator, which is imaged via a pinhole array onto a gated framing camera (GXD). This provides a series of radiographic in-flight images of the ablator within about 500ps of the peak compression, with an example of data shown in panel on lower left of Fig. 19. The dark ovals show compressed ablator while the bright regions in the center of the images are from capsule self-emission. This important diagnostic provides insight into the deleterious effects of the capsule support tent, seeding a hydrodynamic instability which led to non-uniform implosion and mixing of ablator into the fuel and hot spot helping to explain the sub-optimal performance of the NIC implosion designs.

Over the course of FY19 the single line of sight imaging diagnostic (SLOS), which is one of the nine NDWG transformational diagnostics, replaced the gated x-ray imagers as the detector for 2D x-ray backlit imaging (2DCONA). Coupling this new diagnostic with a mono-chromatic imaging crystal (CBI-SLOS) enabled ablator radiography measurements to overcome the capsule self-emission within ~100ps of bang-time, as shown in panel on upper left. It is the narrow bandwidth of the imaging crystal that allows greater discrimination between back-lighter x-rays over the broad-band capsule self-emission, enabling ablator measurements late in the implosion, which could not be done with the previous 2DCONA technique. This new data is currently being used to infer mixing of ablator material into the hot spot, providing valuable new information on an important ICF degradation mechanism. Implosion trajectory and ablator density are also measured using one dimensional x-ray backlighting techniques, which use x-rays to project a 1D slit image onto an x-ray streak camera (DISC).

Another important diagnostic is the one-dimensional velocity interferometer (1D VISAR) that is used to characterize materials at high pressure (as shown in lower middle panel in fig.18) and to synchronize the shocks driven by the x-ray drive through both the capsule and the DT fuel. This ensures that the laser pulse drives the correct sequence of shocks to assemble the fuel. In 2019 NIF diagnostics began the process to develop a new 2D VISAR system on NIF (2DHRV). This is building on the successful OMEGA High Resolution Velocimeter (OHRV) diagnostic, which has been used to study laser driven shock non uniformity, driven by ablator microstructure, on samples of plastic, beryllium and diamond. This diagnostic, which is described in detail in the transformational section **IIIb-7**, uses multiple laser pulses to provide a snapshot of the shock uniformity in the ablator with m/s velocity resolution, and will be used to measure shock uniformity at high pressures obtained in ICF implosions on the NIF. The MJ yield shot in Aug 2021 showed that this diagnostic needs to be placed in a room that is far enough from the chamber and shielded from high neutron fluxes to prevent neutron damage to the detectors. The facility mods required for this will move the completion date of this project towards the end of FY26.

2.3. Stagnation Local diagnostics:

As the capsule approaches peak compression, the hot spot begins to approach maximum density and temperature conditions and produces copious neutrons and x-rays. These particles and photons are used to diagnose stagnation conditions ~100-200ps around time of peak compression. As shown in Fig.17, a large number of diagnostics were commissioned on NIF to characterize stagnation conditions during the NIC. Since then, there have been multiple advances that are greatly improving understanding of these challenging implosions. Some notable examples are; (1) the use of 5 neutron time of flight detectors to provide high precision measurements of neutron ion temperature and the bulk velocity of the neutron emitting hot spot; (2) the use of the multi-kJ, 30ps ARC laser to provide a higher energy X-ray backlight images of the compressed fuel at stagnation, via Compton scattering; (3) multiple Neutron and X-ray imaging lines of sight to provide 3D reconstructions of the neutron and x-ray emitting volume at stagnation. These diagnostics provide powerful new insights into degradation mechanisms that prevent ICF implosions from reaching

their designed performance, these mechanisms are described in detail within the ICF 2020 report.

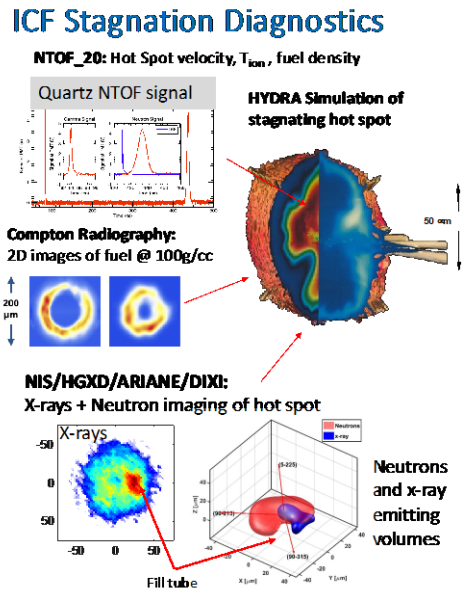

Acronym	Diagnostic	Observable	Category
ARIANE	Hardened Gated x-ray Imager - Chamber based	X-ray hot spot size and shape for yields >2x10^{16} neutrons	NIC
HGXD	Hardened Gated X-ray Detector - DIM based	Ablator symmetry Yn <2x10^{16}	NIC
DIXI	Dilation x-ray imager	X-ray hot spot size and shape with 10ps gate time	NIC
MRS	Magnetic Recoil spectrometer	time history of neutron emission	NIC
Well_NADS	Nuclear activation	Absolute neutron yield	NIC
GRH	Gamma Reaction History	Neutron bangtime and burnwith	NIC
RTNADS	Higher Resolution Unscattered neutron yield	Fuel symmetry	FY19
NIS	3D Neutron Imaging system (3x LoS)	hot spot size and fuel asymmetry 3 axis	FY19
NIS_DS	Second DS LoS	Fuel asymmetry	FY20
NTOF_20_PL	neutron time of flight (5xLoS)	Ion Temperature, hot spot velocity	FY20

Figure 20: ICF Capsule stagnation Diagnostics, showing a hydra simulation of a capsule at bang-time, three examples of important diagnostic measurements; neutron time of flight (NTOF_20), Compton scattering imaging of the dense DT fuel and combined 3D and x-ray imaging neutron imaging of the stagnating hot spot.

Key Stagnation local diagnostic developments in FY22:

Polar DIXI/ARIANE: X-ray emission diagnostics that have been hardened against the high neutron and hard x-ray fluxes are used to measure the shape and brightness of the hot spot throughout the time of peak x-ray emission. HGXD (70ps resolution x-ray framing camera) and Polar DIXI (10ps resolution, x-ray framing camera), are used for this measurement up to neutron yields of 2x10^{16}. ARIANE is a hardened x-ray framing camera placed 6m from chamber center that is designed to provide similar x-ray shape data for yields at ~1x10^{17} neutrons. The MJ yield shot of N210808 (Yn ~4e17) showed that this diagnostic should be able to produce useable data up to about 1e18 neutrons.

Upgrade of NIS_1: This is part of the LANL neutron imaging diagnostic. This diagnostic now produces images of the primary neutron source, down-scattered neutrons that have been down-scattered by the DT fuel and the gamma rays produced by neutrons interacting with the carbon ablator. This now allows measurements of the shape of the neutron emitting hotspot, the DT fuel and the carbon ablator. 23.

GRH/GCD: The Gamma Reaction History (GRH) and Gas Cherenkov Detector (GCD) are both LANL diagnostics that are used to measure the time of peak emission and neutron burn duration which are measured via fusion induced gamma emission using GRH. This measures peak emission time to ±50ps and burn duration to ±30ps. A new diagnostic based on time dilation technology (GCD) has been developed to improve burn width resolution to ~10ps. This began to produce data in 2021 but is affected by fluorescent backgrounds from the gas in the GCD cell. In FY22 we worked on adding a 10ps resolution PDPMT to one arm of GRH to try to overcome this effect

and produce a higher resolution gamma measurement that could give a true burn history rather than a burn width. This will be tested towards the end of Q1 FY23.

RTNADS: Absolute neutron yield is measured using zirconium Nuclear Activation Detectors (Well_NADS). DT fuel uniformity is also measured by a distribution of chamber nuclear activation detectors (RTNADS). In FY20 RTNADS began to provide automatic analysis of low mode fuel uniformity with higher sensitivity and ~2x increased locations (~ 40 vs 18), which allows fuel maps to be measured with higher Legendre modal content (L<4) than the previous FNADs system (L<2). This detector is now run routinely on all high yield shots on NIF. However the LaBr detectors induced a background that takes time to decay. This puts a constraint on the amount of time between high yield DT shots (~ 2 weeks) for this background to die away before the next high yield shot. In FY23 we will work on a lower background RTNAD prototypes that could be used more frequently than the existing LaBr scintillators and photomultipliers.

NTOF_20: A suite of five Neutron Time of Flight systems (NTOF_20; each ~20m from the center of the chamber) are used to measure the ion temperature and hot spot bulk velocity via broadening of the neutrons emitted from the hot spot at time of peak compression. These diagnostics have been developed via a decades long collaboration with scientists and engineers from LLNL, LLE, LANL and Sandia. Fig.17 shows example data from a new high temporal resolution quartz detector. In addition to Ion temperature and bulk velocity these powerful diagnostics also measure the fraction of neutrons that are down-scattered by the DT fuel (the Down Scattered ratio = DSR), giving 5 measurements of fuel density around the implosion. The five NTOFs with the high temporal resolution quartz detectors are now routinely used to measure the bulk velocity of the hotspot velocity (giving resolution of <5km/s).

4. Local diagnostics supporting HED science experiments on NIF:

The diagnostic suites support experiments that generate weapon-relevant HED conditions in specialized laboratory environments for NIF, Omega and Z. These are generally experiments that use a subset of the facility diagnostics to study focused physics problems relevant to weapons science in the general areas of radiation flow and material properties at high pressures (including equation of state, opacities, and material strength) as shown in Fig. 21. On NIF the VISAR system is used for shock timing in ICF implosions, and for equation of state studies that have provided important data on a range of materials for the national HED program. Planned improvements to the VISAR system on NIF will allow extremely precise measurements of pressure profiles and will provide a new capability to study shock uniformity in materials of interest to the HED community by the end of FY23. X-ray diffraction is another important diagnostic that is used to directly measure the crystal structure, adding another constrain to the equation of state in HED experiments. On NIF the TARDIS diagnostic is used to characterize the crystal structure of important materials at high pressures.

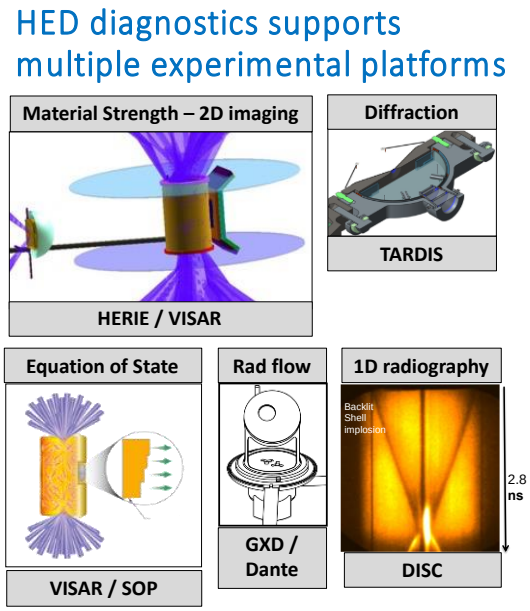

Acronym	Diagnostic	Observable	Category
VISAR	Velocity Interferometer for any reflector	shock velocity vs time	NIC
SOP	streaked optical pyrometer	temperature diagnostic for shock materials	NIC
DISC	DIM Insertable (x-ray) Streak camera	soft x-ray imaging and Spectroscopy	NIC
SXI	x-ray imager for hohlraum imaging	Hohlraum laser entrance hole closure	NIC
HERIE	passive hard x-ray imager	image plate based imaging snout	NIC
GXD	Time gated x-ray Detector	Soft x-ray imaging, Radiation flow	NIC
DANTE 1	Broadband, time-resolved x-ray spectrometer	Hohlraum x-ray conditions	NIC
RADChem	gaseous and solid radchem	collect and count activated samples from implosions	NIC
DANTE 2	Broadband, time-resolved x-ray spectrometer	Hohlraum x-ray conditions	Post NIC
VIRGIL	soft x-ray spectrum	Hohlraum x-ray conditions	Post NIC
TARDIS	X-ray Diffraction	crystal strucure	Post NIC
EXAFS	Edge x-ray absorption fine structure	Temperature diagnostic for shocked materials	FY20

Figure 21: The NIF diagnostic suite supports focused science experiments for the HED program, some of the many examples are shown here. These include advanced 1D streaked x-ray radiography using DISC, 2D high energy radiography for material strength using image plates (future experiments will use ARC and high energy HCMOS gated detectors), material behavior at ultra-high pressures with VISAR, SOP, TARDIS, EXAFS and DIFF(t).

In FY22 a prototype time resolved version of TARDIS, called G3D using SNL supplied Icarus hCMOS detectors has produced multiple frames of diffraction data (with 1.5ns temporal resolution) on a single shot. In FY23 we plan to commission a version, called FIDDLE that has more sensors with higher well depth (SNL supplied Daedalus devices). This is being designed to produce more frames per experiment and is due to provide data by late FY23. Gated x-ray framing cameras (GXD) are also used to diagnose radiation flow via plasma self-emission and x-ray streak cameras (DISC) are used to measure material equation of state through 1D streaked x-ray radiography on both NIF and OMEGA. Material strength at high pressure has been successfully measured using point projection x-ray backlighting and simple image plate diagnostics. In the future this experiment capability will be extended to thicker samples by using ARC or OMEGA EP to drive higher x-ray energy back-lighters. These techniques will be used to diagnose metallic ablator conditions that are relevant for double shell implosion science. The data return per experiment can be increased by using gated high energy hCMOS detectors (DHEX/HEXI) to obtain multiple frames per shot. New cathode materials that are sensitive to more energetic x-rays (>15keV) will be required for these devices. R&D work is underway on Germanium and GaAs detectors that can provide good detection efficiency for these x-ray energies.
In FY22 we also commissioned EXAFS spectrometers which are used to measure the spectral modulations near a K or L edge in materials that have been compressed to high pressures. These spectrometers, which have been developed in collaboration with PPPL, utilize novel x-ray crystal geometries to enable high throughput with high

spectral resolution. In FY22 we commissioned 3 systems to measure Cu K shell, Tantalum L shell and Lead L – shell. Future work in FY23/24 will develop crystals that can diagnose EXAFS around the Pu L shell.

With the development of volume burn platforms that utilize opaque metal shells (pushered single shells and double shells), diagnostics capable of constraining high-Z mix are needed. Since x-rays do not escape these shells all information about the stagnation phase must use nuclear techniques. Leading detection methods of mix use charged-particle radiochemical and reaction-in-flight (RIF) neutron spectral measurements. The radiochemical products must be efficiently collected and then counted to understand the levels of mix that occurred. These capabilities exist at NIF, but must be regularly maintained and improved for future use.

V-2: Local Diagnostic Development on Z

The development of new local diagnostic capabilities on Z is aimed at improving the fidelity by which we can measure time-dependent phenomena in all our HED platforms with an emphasis on the needs to understand stagnation dynamics in magnetic direct drive ICF. Development activities in FY22 were focused on:

- X-Ray Diffraction
- Gamma Reaction History (With LANL, LLNL, & NNSS)
- Compact Recoil Spectrometer (With MIT)
- SCORPIONZ streak camera (With LLNL)
- Precision nToFs (with LLNL)
- 2D Neutron Imaging (with LLNL and LANL)
- Development of an equatorial line of sight
- Expansion of Line VISAR capabilities

In the next few years more dedicated efforts will be placed on neutron diagnostics that will be enabled by tritium operations on Z. Table 5 shows the present estimates of the timeline for development of the local diagnostics on Z.

Brief description of these capabilities and their applications:

MONSSTR: Multi Optic Novel Spherical Spectrometer with Time Resolution is a time gated in-chamber spectrometer being developed to diagnose the evolution of mix in ICF experiments. Future plans include integrating tiled Daedalus sensors to increase the spectral range.

Multi-Frame Crystal Backlighting: This is a spherical crystal backlighter coupled to an hCMOS camera with multiple laser pulses to enable multi-frame capabilities. The primary application is measuring the liner mass distribution near stagnation in MDD-ICF.

High energy and faster diodes: This work supports both increasing the temporal response and development of higher energy diodes. The primary application is measuring the time-dependent x-ray output spectrum from >15 keV x-ray sources. Ongoing research involves GaAs, CdTe, and 100um thick silicon.

GRH-Z: This is a gamma reaction history diagnostic to measure the time-history of the DT fusion production in MDD-ICF (requires ~1% tritium on Z). Future plans include improving gamma shielding and incorporating a PDPMT to improve the temporal response.
SCORPIONZ, X-Ray Streak Camera – Streak Camera Observatory for Radial or Polar Implosions ON Z. Enables much faster temporal response to better understand evolution of target parameters. In FY21 a conceptual design was held in collaboration with LLNL.

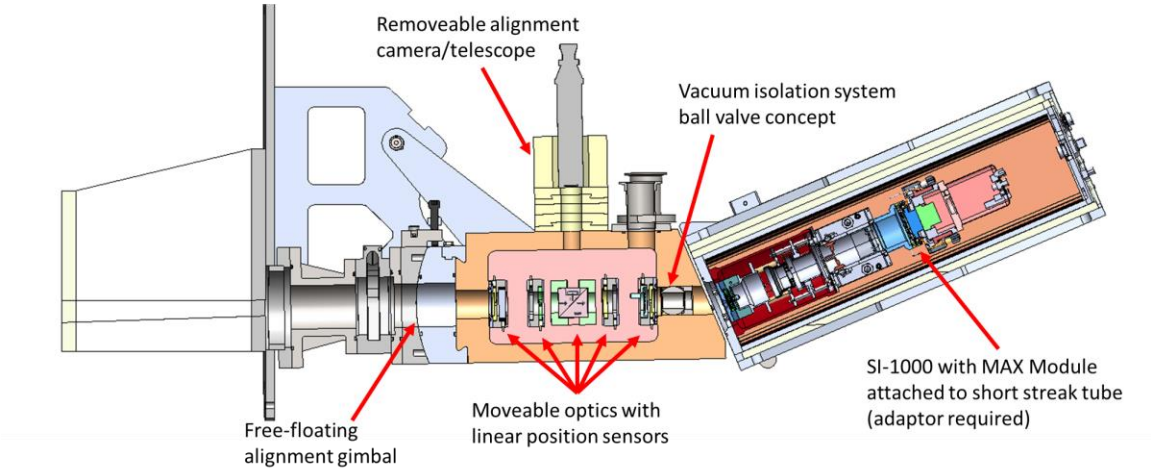

Figure 22 Cross section of SCORPIONZ diagnostic in Z Diagnostic Boat

Precision nTOF – Developing an advanced nTOF system that will use three equatorial line of sight.
2-D Neutron Imager: This is a time-integrating 2-D neutron imager optimized for primary DT neutrons from the stagnation in MDD-ICF.
Temperature Diagnostics for Materials Research: This is part of multi-year effort to diagnose the temperature of dynamically compressed material samples. Infrared and Near Visible Pyrometry, Infrared Reflectance, and reflectance spectroscopy are being developed.
X-Ray Diffraction – Measure the phase dynamics of compressed materials for Materials Research.
Equatorial Line of Sight – A new diagnostic capability that will allow an equatorial view of imploding targets from distances greater than 3m. The transport section will extend through the water and oil sections of Z which will provide great neutron

collimation for future nuclear diagnostics.

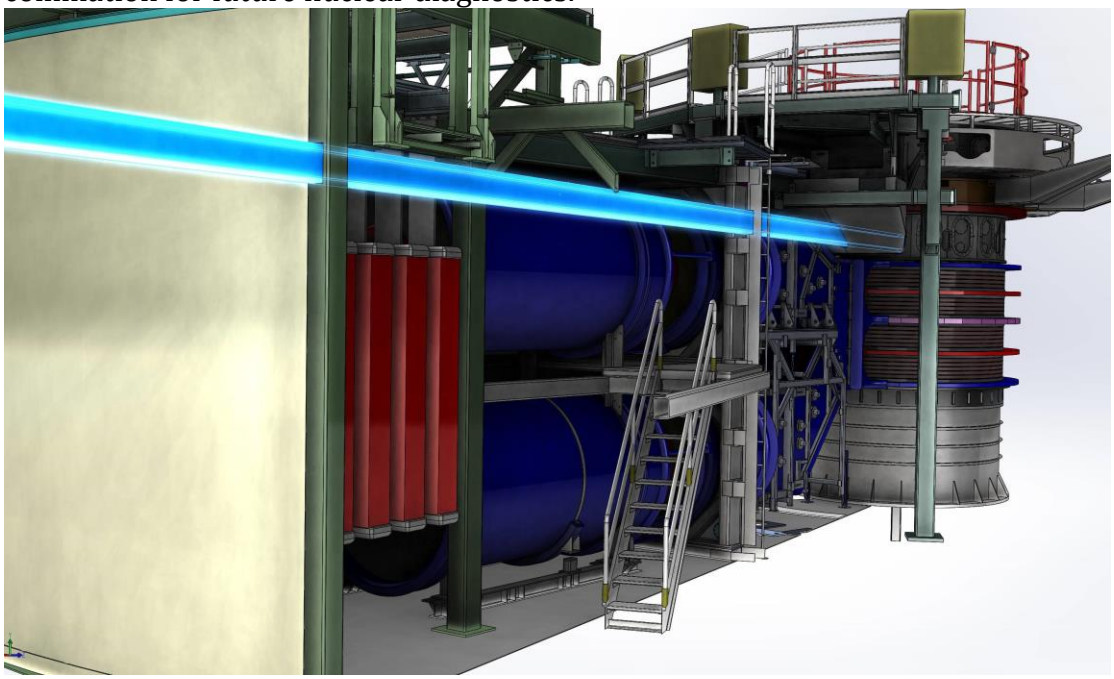

Figure 23 View of equatorial line of sight extending through the pulsed power sections of Z.

Line VISAR– In FY21 the Line VISAR system, developed in collaboration with LLNL, continues to expand to other experimental campaigns and expanding its capability to image plasma formation that could lead to current loss in Z.

Major Z Local Diagnostic	Status	FY21				FY22				FY23				FY24			
		Q1	Q2	Q3	Q4	Q1	Q2	Q3	Q4	Q1	Q2	Q3	Q4	Q1	Q2	Q3	Q4
MONSSTR	In Progress																
Multi-Frame Backlighting	In Progress																
High Energy & Faster Diodes	In Progress																
Gamma Reaction History-PDPMT	Not Started																
Compact Recoil Spectrometer	In Progress																
RadChem	In Progress																
SCORPIONZ	Development																
Precision nToF	Development																
2D Neutron Imager	Development																
Temperature Diagnostics for Material Research	In Progress																
X-Ray Diffraction	In Progress																
Equatorial Line of Sight	Development																

Table 5: Estimated timelines for the local diagnostic effort on Z.

Z has a diverse portfolio of experimental platforms that support multiple experimental campaigns. For Magnetic Direct Drive Fusion experiments the MagLIF concept is used and shown in Figure 21. Recent efforts have focused on understanding current delivery (Z Line VISAR) and stagnation diagnostics; need to implement 1) 2D neutron imager, 2) fusion burn history measurement, and 3) time gated spectroscopy and imaging. There are existing limitations that don't allow backlighting and MagLIF to be executed simultaneously or Backlighting and Line VISAR.

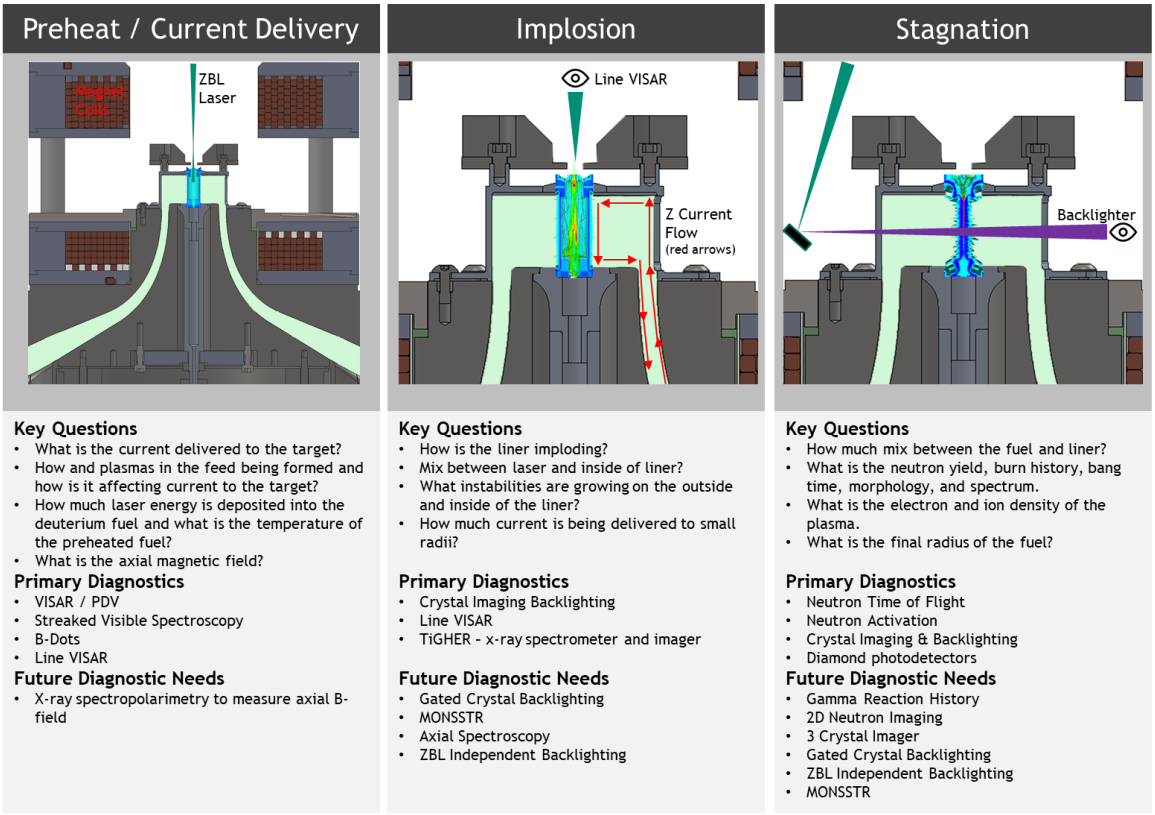

Figure 24: Magnetic Direct Drive implosion experiments are diagnosed to understand fundamental target physics in three general phases. Cross-section of the MagLIF hardware.

Local Diagnostic Effort on OMEGA

Introduction: Scientific advances in High Energy Density (HED) physics are realized with an innovative research and development program of visible, ultraviolet, x-ray, gamma ray, nuclear, and particle diagnostics. Inertial Confinement Fusion (ICF) and the pursuit of ignition has been a major driver for diagnostic development for decades and this has driven many advances in diagnostics that are now being used in the wider HED community. The development of many diagnostics for Laser Indirect Drive (LID), Magnetic Direct Drive (MDD) and Laser Direct Drive (LDD) on the National Ignition Facility (NIF) often starts with a prototype demonstration on the Omega Laser Facility. There is also strong synergy between diagnostic groups at the major HED facilities: OMEGA, Z and NIF. It is coordinated through quarterly meetings of the Leadership Team for the National Diagnostics Working Group, which LLE is an active participant.

The Omega Laser Facility is used to develop diagnostics for the three ignition approaches in ICF and HED experiments. LDD ICF implosions and focused HED experiments on OMEGA are diagnosed to understand fundamental target physics. For ICF the key target physics areas for each of the four phases of a LDD implosion—initial plasma formation, acceleration phase, deceleration phase, and stagnation—are highlighted in Fig. 1, including laser drive uniformity, laser imprint, laser plasma instabilities, energy coupling, shock propagation, hydrodynamic instabilities, hot-electron preheat, multidimensional effects on hot-spot formation, and residual kinetic energy. A multi-year research and development

effort is being conducted for 3-D (i.e., having three or more diagnostic lines of sight) x-ray and nuclear diagnostics to study multidimensional effects on LDD implosions during the all phases of the implosion. The development of primary diagnostics, including the accuracy and precision requirements, are derived from the fundamental target physics needs. In addition, the high shot rate on OMEGA and OMEGA EP is exploited to develop LID and MDD diagnostics for NIF and Z, respectively.

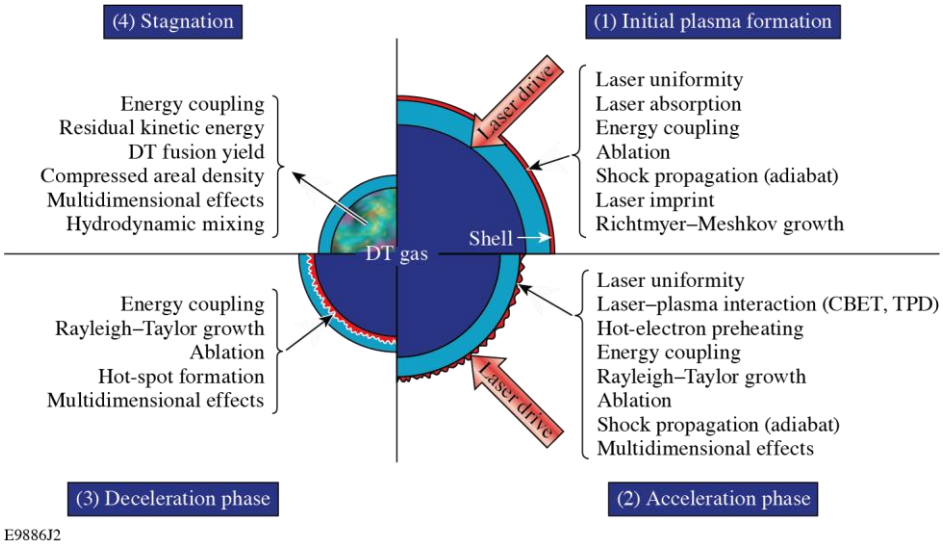

Figure 25. The key target physics areas for each of the four phases of an LDD implosion

The primary diagnostics associated with the key target physics of the initial plasma formation and the acceleration phase of an LDD implosion are listed in Table 6. Many synergies were realized with the VISAR diagnostic, which is used by all three approaches. Diagnostics developed for NIF on OMEGA are highlighted with an asterisk.

Target physics area	Diagnostic and measurement
Laser Uniformity	Full-beam in-tank diagnostic (records the spatial distribution of UV far-field fluence inside the OMEGA target chamber) [1] X-ray target plane (infers the spatial distribution of UV far-field fluence from x-ray spots recorded on target) [2] Fixed x-ray pinhole cameras for beam pointing [3] Laser power balance measurement [4] Ultraviolet equivalent target plane [5]
Laser Absorption	Full-aperture backscatter station for time-resolved scattered light spectroscopy [6] Scattered Light Uniformity Imager (SLUI)
Ablation/Shock Propagation/adiabat	1-D VISAR (velocity interferometer system for any reflector) [7]* Refraction-enhanced X-ray radiography [8] X-ray Thomson Scattering [9] X-ray Talbot-Lau deflectometry [10]
Laser Imprint/Richtmyer–Meshkov Growth	OHRV (2-D VISAR) [11]* Through-foil x-ray radiography [12]
Laser Plasma Instabilities	Full-aperture backscatter station for time-resolved scattered light spectroscopy [6] 3/2ω time- and space-resolved imagers [13]

	2ω and 4ω (5ω in future) optical Thomson scattering [14]* 4ω interferometry [15] and angular filter refractometry [16] TOP9 beam and transmitted-beam diagnostic [17] Angularly-Resolved Thomson Scattering for electron distribution functions [18] Hard x-ray diagnostic [19]
Energy Coupling	Shell trajectory measurements using x-ray framing cameras (XRFC) [20]
Rayleigh–Taylor Growth	Through-foil x-ray radiography using Fresnel Zone Plates [21]
Multidimensional Effects	3-D in-flight ablation surface measurement using XRFC [22]

Table 6. LDD key target physics areas and diagnostics for the initial plasma formation and acceleration phase. *These diagnostics were developed on OMEGA for NIF through collaborative efforts amongst scientists and engineers from LLE, LLNL, LANL, SNL, MIT, Kentech and the NDWG.

The primary diagnostics associated with the key target physics of the deceleration phase and stagnation of an LDD implosion are listed in Table 7. Diagnostics developed for NIF on OMEGA are highlighted with an asterisk.

Target physics area	**Diagnostic and measurement**
Hot-spot formation/ Multidimensional Effects / Hot-spot flow velocity	3-D gated x-ray imaging of hot spot [23] 16 channel gated Kirkpatrick–Baez microscope [24] Single line-of-sight time-resolved x-ray imager (SLOS-TRXI) [25]* 3-D neutron time-of-flight (nTOF) detectors [26]* Neutron imaging [27]* Penumbral imaging of knock-on deuterons (KoDI) [28] X-ray backlighting with monochromatic crystal imager at 1.86 keV [29] Spec T_e [30] or x-ray penumbral imager [31] particle X-ray temporal diagnostic (PXTD) to diagnose hot-spot T_e [32] High-resolution X-ray spectroscopy [33]*
Hydrodynamic Mixing	X-ray spectroscopy of high-Z dopants [34]* X-ray backlighting with monochromatic crystal imager [29] Comparison of absolute x-ray continuum emission (Spec T_e) and neutron yield from hot spot [35]
Fusion Yield	nTOF detectors (yield, T_i) [26]*, [36]* Cu activation detector [37] Neutron bang time and burn rate [38] PXTD [32]
Compressed areal density	Charged-particle spectrometer [39] Neutron spectroscopy via nTOF detectors in shielded and collimated diagnostic lines of sight [40] and magnetic recoil spectrometer [41]* X-ray backlighting with monochromatic crystal imager at 1.86 keV [30] Compton Radiography [42]* KoDI [28]

Table 7. LDD key target physics areas and diagnostics for the deceleration phase and stagnation. *These diagnostics were developed on OMEGA for NIF through collaborative efforts amongst scientists and engineers from LLE, LLNL, LANL, SNL, MIT, GA, Kentech, Sydor Technologies, and the NDWG.

In support of high energy density physics experiments conducted on the Omega Laser Facility, the National Ignition Facility, and advanced light sources, LLE pursues diagnostic developments for the following research thrusts: studying fundamental high energy density physics (i.e., equation of state, opacity, conductivity, stopping power, and viscosity), developing innovative diagnostic techniques for HEDP (e.g., THz spectroscopy, Raman Spectroscopy, streaked optical pyrometry spectrometers, high-resolution x-ray spectroscopy, and superconducting superfluid detection), and the development and application of probes for HEDP (e.g., THz radiation, X rays, Hard X rays, γ-rays, and

particle beams). The OMEGA EP PW laser, similar to Z-beamlet and ARC, is combined with OMEGA to develop advanced x-ray and particle probe sources for HED plasma research. The primary diagnostics associated with high energy density physics experiments conducted at OMEGA are listed in Table 8. Diagnostics developed for NIF on OMEGA are highlighted with an asterisk.

Target physics area	**Diagnostic and measurement**
Equation of state	1-D VISAR (velocity interferometer system for any reflector) [7]
Opacity	X-ray spectroscopy of high-*Z* dopants [34]* X-ray backlighting with monochromatic crystal imager [29] High-Resolution Spectroscopy [33]* Imaging X-ray Thomson Scattering [43]
Conductivity	Streaked Optical Pyrometry [44] Streaked Spectral Pyrometry [45]
DC conductivity, phonon states, molecular structure	THz spectroscopy [46]
Stopping Power	Charged Particle Spectrometer [39]* Wedge Range Filter Module [47]* Magnet Recoil Spectrometer [41]*
Viscosity	1-D VISAR (velocity interferometer system for any reflector) [7]
Long-range Ordering	Powder X-ray Diffraction Image Plate (PXRDIP)* [48]

Table 8. HED key target physics areas and diagnostics. *These diagnostics were developed on OMEGA for NIF through collaborative efforts amongst scientists and engineers from LLE, LLNL, LANL, SNL, MIT, GA, Kentech, Sydor Technologies, and the NDWG.

Progress in FY23: In FY23 several research and development efforts for diagnostics on the Omega Laser Facility were performed. They are summarized in the table shown in Table 9. Some of them involved collaborations with members of the NDWG from LLNL, SNL, MIT, Sydor, GA, and Kentech. Refurbishment activities included finding a replacement sensor for the obsolete Charge Injection Device (CID) detectors and the replacement of the two Active Shock Break Out (ASBO) laser systems for OMEGA and OMEGA EP. Novel diagnostic development includes the Particle and x-ray temporal diagnostic (CryoPXTD), the OMEGA X-ray Hot-Spot Imager (XRHSI), simultaneous VISAR and X-ray Radiography on OMEGA EP, and the development of a 4π average compressed areal density diagnostic.

Diagnostic	**Status**	**Collaborating Lab**
Active Shock Break Out (1-D VISAR)	Two new diode pumped solid-state laser systems have been designed and are being procured for replacement on OMEGA and EP to ensure continued availability of the VISAR system in FY24 and beyond	LLNL
CryoPXTD*	New scintillator array developed to simultaneously record DT-neutrons, two x-ray channels and D-3He protons to assess kinetic effects in implosions.	MIT
Long Term replacement for X-ray Pinhole camera detectors*	Prototype replacement system has been procured and is being configured for ride-along experiments in FY24.	SNL, Sydor

4π ρR (3-Dimensional nTOF) [49]*	Collaboration with Imperial College on MCNP simulations to determine most effective locations of additional required collimated lines-of-sight. LLE held internal workshop to refine the analysis techniques and compare different diagnostic modalities (e.g. NTOF, MRS) for assessment ρR.	LLNL, Imperial
OMEGA X-ray Hot Spot-Imager (XRHSI) [50]	Photocathode pulser and pulse delivery structure has been built and qualified to perform to specification. LLE anticipates receiving the pulser at the end of FY23. Project continues into FY24 with multi-meter drift tube design and assembly. Integration onto OMEGA chamber is expected later FY24.	LLNL, SNL, GA, Kentech, Sydor
3-D reconstruction of hot-spot formation [23]	Novel 3-D reconstruction algorithms using hot-spot x-ray images recorded along three or four diagnostic lines of sight have been developed. Low-mode reconstructions of the hot-spot are being studied.	LANL, LLNL
Raman Spectroscopy on OMEGA [51]	Raman spectroscopy to directly measure, for the first time, novel chemistry phenomena at HED pressures, crystallographic structure of low Z materials, and temperatures lower than what is accessible to streaked optical pyrometry.	LLNL
Simultaneous VISAR and X-ray Radiography on EP	A new optical transport has been designed to enable face-on, short-pulse x-ray radiography in tandem with VISAR particle velocity measurements on OMEGA EP. This capability is anticipated in Q2 FY24.	LLE, LLNL

Table 9. Local Diagnostic Projects underway and proposed at OMEGA. *These diagnostics were developed on the Omega Laser Facility through collaborative efforts amongst scientists and engineers within the NDWG from LLE, LLNL, LANL, SNL, MIT, GA, Kentech, and Sydor Technologies.

Diagnostic Name	**Diagnostic Status**	**Lead Lab**	**Diagnostic description**
Omega High Resolution Velocimeter (OHRV)	Operationally Qualified	LLE/LLNL	Operationally qualified and operated on two OMEGA shot days in FY23. LLNL supplied a new laser front end integrated into the OMEGA laser bay. LLNL and LLE are working to transfer operations, specialist, and data analysis responsibilities onto LLE staff.
Polarization Resolved Ultraviolet Thomson Scattering [52]	Preliminary Qualified	LLNL	This design uses a Wollaston prism to simultaneously separate signal polarizations and disperse the UV light. Signal polarization is aligned with one channel, improving signal/background by a factor of two. A second channel provides an independent measurement of background, allowing a full background subtraction of unpolarized thermal emission.

Multi-frame Zoneplate Imager	Operationally Qualified	LLE	A system consisting of an hCMOS sensor on OMEGA coupled to a Fresnel zone plate imaging system. LLE is collaborating with SNL on fielding the hCMOS on the Fresnel Zone Plate imager to achieve ns-resolution for hydrodynamic instability experiments.
Full Aperture Backscatter-P9	Preliminary Qualified	LLE	Refurbishment project of the OMEGA backscatter station. New spectrometers were procured in FY23 and two ROSS streak camera systems were upgraded with optical calibration modules to integrate with the new spectrometers.
Electron Spectral Imager	Operationally Qualified	LLE	Designed to collect wide-angle (~120^{o}) electron spectrum from short-pulse driven micro-channel targets. Adapted from a design fielded at Texas Petawatt
Spectroscopy Resolved Streaked Optical Pyrometer	Preliminary Qualified	LLE	With the addition of spectral resolution, the proposed SOP-Spec will be capable of measuring temperature down to 3000K, and wavelength dependent emissivity and reflectivity of compressed materials in the ~400-850 nm range with ~100 ps temporal resolution.

Table 10. Diagnostics qualified on the Omega Laser Facility in FY23. The diagnostic name, diagnostic status, lead lab, and diagnostic description are listed in the table.

In FY23 a number of novel local diagnostics were qualified for use on the Omega Laser Facility. They are listed in the table shown in Table 10 along with the diagnostic status, lead lab, and diagnostic description. Several notable qualification experiments with their data follow below.

In collaboration with LLNL and SNL, LLE has successfully developed and implemented an hCMOS sensor on OMEGA coupled to a Fresnel zone plate imaging system. Figure 1 shows two successive radiographs measured 4-ns apart where the Rayleigh-Taylor growth of a blast-wave-driven, two-mode interface between a plastic pusher and a low-density foam was observed on a single shot with a temporal resolution of ~100 ps and a spatial resolution of a few microns. Target development activity was carried out in collaboration with the University of Michigan and SciTech. This is a unique demonstration of coupling an hCMOS detector to a Fresnel zone plate radiography platform in a high-energy density environment by another successful multi-institutional collaboration.

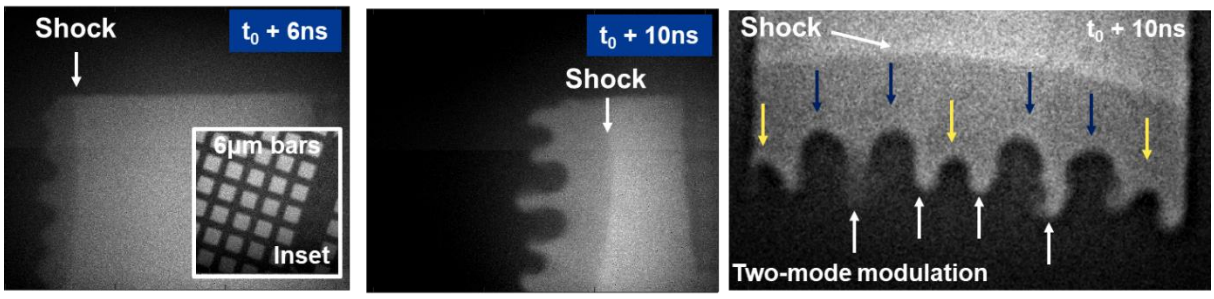

Figure 26. Evolution of shock-driven blast waves and Rayleigh-Taylor bubble growth recorded using the Multiframe Zoneplate Imager Diagnostic. Two-mode sinusoidal modulations were imposed between the plastic pusher and low-density foam in which the instability was observed to grow.

LLE successfully carried out a preliminary qualification shot day on OMEGA EP for the SOP-Spec diagnostic, where the team measured spatially-integrated, time and spectrally-resolved, broadband pyrometry measurements from laser-driven quartz, fused silica, and diamond targets at a variety drive conditions. A representative streaked spectra obtained from the driven diamond target is shown in the Figure 27. Broadband pyrometry will enable improved temperature measurements without reliance on the grey-body model and at lower temperatures. The diagnostic will enable additional advancements in understanding emissivity and absorptivity of ramp-compressed HED materials.

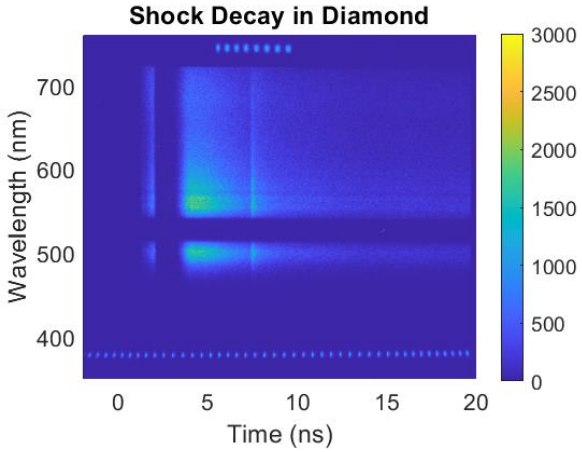

Figure 27. Streaked spectrum obtained from the SOP-Spectrometer instrument activated in FY23.

A new four-channel scintillator for the CryoPXTD instrument was fielded on a qualification campaign on OMEGA, focusing on multi-ion and other kinetic effects in thick-shell hoppe glass implosions. The experiments observe the D-$_3$He protons, DD-neutrons, DT-neutrons and x-ray temporal evolution with individually filtered channels. Data obtained from the CryoPXTD streak camera are shown in the left panel of Figure 28 and the summed channel signals are plotted against emission time in the right panel.

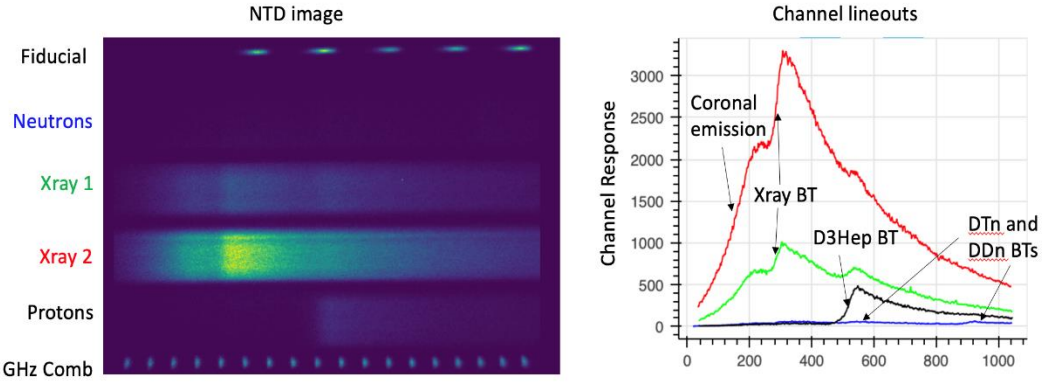

Figure 28. Data obtained on OMEGA campaign MULTIION-23A in support of qualification of the CryoPXTD diagnostic. The four-channel streaked image shows the ability to simultaneously record

implosion generated D-$_3$He protons, DT-neutrons and X-rays within the streak camera's dynamic range for a single shot.

References

[1] L. J. Waxer et al., Proc. SPIE 10898, 108980F (2019).
[2] W. Theobald et al., RSI 91, 023505 (2020).
[3] R. Forties and F.J. Marshall, RSI 76, 073505 (2005).
[4] S. Sampat et al., Applied Optics 57, 9571 (2018).
[5] S. P. Regan et al., JOSA B 17, 1883 (2000).
[6] W. Seka et al., POP 15, 056312 (2008).
[7] P. Celliers et al., RSI 75, 4916 (2004).
[8] A. Kar et al., POP 26, 032705 (2019).
[9] S. P. Regan et al. PRL 109, 265003 (2012).
[10] M. P. Valdivia et al., Appl. Opt. 57, 138 (2018).
[11] P. Celliers et al., RSI **81**, 035101 (2010); Peebles et al., PRE 99, 063208 (2019).
[12] V. Smalyuk et al., PRL 81, 5342 (1998).
[13] W. Seka et al., PRL 112, 145001 (2012).
[14] I.A. Begishev et al., Optics Letters 43, 2462 (2018).
[15] A. Howard et al., Rev. Sci. Instrum. 89, 10B107 (2018).
[16] D. Haberberger et al., Phys. Plasmas 21, 056304 (2014).
[17] D. Turnbull et al., Nature Physics 16, 181 (2020).
[18] A.L. Milder et al. POP 26, 022711 (2019).
[19] W. Stoeckl et al., RSI 92, 1197 (2001).
[20] P. Michel et al., RSI 83, 10E530 (2012).
[21] F.J. Marshall et al. submitted for publication.
[22] P. Michel et al., PRL 120, 125001 (2018).
[23] K. Churnetski et al., RSI 93, 093530 (2022).
[24] F.J. Marshall et al., Rev. Sci. Instrum. 88, 093702 (2017).
[25] W. Theobald et al., RSI 89, 10G117 (2018).
[26] O.M. Mannion et al., Nucl. Instrum. Methods Phys. Res. Sect. A 964, 163774 (2020); O. M. Mannion et al., Rev. Sci. Instrum. 92, 033529 (2021); O. M. Mannion et al., Phys. Plasmas 28, 042701 (2021).
[27] C.R. Danly et al., RSI 86, 043503 (2015).
[28]H. Rinderknecht et al., RSI 93, 093507 (2022); J. Kunimune et al., Phys. Plasmas 29, 072711 (2022).
[29] W. Stoeckl et al., POP 24, 056304 (2017).
[30] D. Cao et al., POP 26, 082709 (2019).
[31] P. Adrian et al., RSI 92, 043548 (2021).
[32] H. Sio et al., RSI 87, 11D701 (2017).
[33] P. Nilson et al., RSI 87, 11D504 (2016).
[34] S.P. Regan et al., PRL 111, 045001 (2013).
[35] T. Ma et al., PRL **111**, 085004 (2013); Epstein et al., Phys. Plasmas **22**, 022707 (2015).
[36] V. Yu. Glebov et al., RSI 81, 10D325 (2010).
[37] O. Landoas et al., RSI 82, 073501 (2011).
[38] W. Stoeckl et al., RSI 87, 053501 (2016).

[39] C.K. Li et al., POP 8, 4902 (2001).
[40] C. Forrest et al., RSI 83, 10D919 (2012).
[41] J. A. Frenje et al., Phys. Plasmas 17, 056311 (2010).
[42] R. Tomassini et al., Phys. Plasmas 18, 056309 (2011).
[43] E. J. Gamboa et al., RSI 83, 10E108 (2012).
[44] J. E. Miller et al., RSI 78, 034903 (2007).
[45] N. Kabadi et al., APS DPP 2022.
[46] G. Bruhaug et al., RSI 93, 123502 (2022).
[47] F. H. Seguin et al., RSI 83, 10D908 (2012).
[48] J. R. Rygg et al., RSI 83,113904 (2012).
[49] C.J. Forrest et al., RSI 93, 103505 (2022).
[50] S. T. Ivancic et al., RSI 93, 113521 (2022).
[51] A. LaPierre et al., APS DPP 2022.
[52] Swadling and Katz, RSI 93, 013501 (2022).

Appendix:

Scattered light diagnostic for direct drive (DD) - five systems: Scattered light diagnostic to measure angular distribution of scattered laser light principally from Direct Drive laser illumination experiments on NIF.
Upgrade DISC: The existing DIM Insertable Streak Camera (DISC) will be upgraded with improved electron optics to improve the spatial resolution over the whole 24mm active area of the cathode. The microchannel plate fiber optic detector will also be replaced with a direct electron detection CMOS detector.
CBI: Crystal Backlit Imaging; this diagnostic uses spherical Bragg crystals to provide narrow band (dE/E < 0.5%) high resolution imaging (<10 micron) at discrete photon energies (6keV – 16keV) for ICF and HED applications.
HGXD-Rad Hard Camera: Replace the optical film that is used in the current Hardened Gated X-ray framing camera Diagnostic (HGXD) with radiation hardened CMOS sensors to increase useful neutron yield ceiling of these x-ray imaging cameras to ~ 10^{17} neutrons per shot.
Z_VISAR: This is 1-D imaging open-beam VISAR system developed in collaboration between SNL and LLNL for use on Z. The primary application is measuring current delivery to MDD-ICF targets.
Prec.nToF/Quartz Detector: Precision Neutron time of Flight diagnostic will replace existing Bibenzyl scintillator as the neutron detector with device using Cherenkov emission in quartz crystals. This fast optical signal reduces the instrument response function (IRF) from its current many nanoseconds to ~350 of pico-seconds. This effectively reduces the DT Tion systematic uncertainty due to the IRF to around 50 eV. Further, since the crystal is also sensitive to gammas produced at bangtime, the detector will also improve the accuracy of fluid velocity measurements by through direct measurement of the neutron-gamma flight time difference along a given flight path.
RTNADS: The real time Nuclear Activation Diagnostic uses in situ Zirconium activation coupled to photomultipliers to provide a real time spatial measurement of the neutron flux at the NIF target chamber after a high yield shot (>5e14 neutrons). This diagnostic

will provide a spatial map of relative un-scattered neutron flux at least 24 locations around the NIF target chamber. This data is designed to be used to infer the uniformity of the compressed DT fuel in an ICF implosion.

Contaminated Control VISAR: This diagnostic modifies the VISAR debris shield so that VISAR can be used whenever NIF is used to study hazardous material such as "high Z".

SPBT upgrade: South-Pole Bang-Time will be upgraded to provide new HAPG crystals and Indium Phosphide detectors that that will characterize the time of peak x-ray capsule emission at both 15 and 30keV. This will be used to obtain a slope temperature measurement at x-ray energies that are transparent to the imploded shell in high convergence implosions.

Crystal calibration facility: X-ray calibration station inside NIF facility, to measure absolute sensitivity and sensitivity vs x-ray energy of NIF spectrometer snouts in the geometry in which they are used and to track performance vs time.

U.V. Interferometry-polarimetry: Optical diagnostic for measure density profiles and magnetic fields in low density plasmas, relevant for discovery science and hohlraum science.

EXAFS spectrometer: High resolution spectrometer for measuring Absorption Fine Structure near absorption edges. This is a sensitive temperature diagnostic in shock heated plasmas. This design allows crystals to be changed to look at the different absorption edges.

DIXI Polar: "Dilation Imager for X-rays at Ignition". A DIXI high temporal resolution x-ray imager will be mounted on the Polar DIM of the NIF target chamber. This diagnostic utilizes a time dilation drift tube to obtain x-ray images of high yield implosions from the pole with a time resolution better than 10 ps. This kind of time resolution is necessary because as the yield increases, the duration of x-ray emission reduces to 100 ps.

Toroidal x-ray imager: Toroidal curved x-ray imaging microscope for quasi monochromatic radiography of plasmas and shocked material with <10um resolution and dE/E ~0.5%

HRV: NIF High Resolution Velocity Interferometer. This is a 2-Dimensional diagnostic for measuring shock uniformity in ICF ablators such as CH, HDC and Be at pressures in 1 to >20 Mbar range with gate times < 40 ps.

Imaging x-ray spectrometer: High spatial and spectral resolution imaging spectrometer for characterizing temperature gradients in HED plasmas.

SPEC5 nToF: 5^{th} Neutron time of flight diagnostic in a location opposite to existing to nToF detectors. This diagnostic will help to increase accuracy of fluid velocities in high convergence ICF and HED implosions

SPEC6 nToF: 6^{th} Neutron time of flight diagnostic in a location opposite to existing to nToF detectors. This diagnostic will help to increase accuracy of fluid velocities in high convergence ICF and HED implosions

VIRGIL time resolved spectrometer: Adding time resolution to the VIRGIL X-ray spectrometer for characterizing hohlraum emission spectrum in soft x-ray regime.

4ω FIDU: This is a replacement for the optical 4ω (263nm) timing Fiducial that serves SPIDER and DISC streak cameras to improve reliability and energy output.

HEXI: The High Energy X-ray Imager is a DIM insertable direct detection diagnostic built using dual hCMOS gated sensors for nanosecond time scale imaging of x-rays in the rang of 10keV to 50keV.
ISS: Will allow x-ray spectra to be recorded along the polar axis with simultaneous neutron imaging and x-ray pinhole imaging; the spectral data will still have 1D spatial resolution and may be recorded in time-resolved snapshots.
NEPPS: A new NEPPS design for use on Cryotarpos or 90-348 for use as a diagnostic for ARC beam studies
SSII: New replacement Qtz or PET crystals in the existing SSII snout to look at backlighter and Compton
AXIS Snout (DRI): New snout to use on ARC dual backlighting on image plate to radiograph large field of view targets. New snout shall leverage existing AXIS snout design.
EHXI 90-110 Electronic Readout: The addition of an electronic readout system for the existing equatorial hard x-ray imager (eHXI) will eliminate the cost and time associated with processing of image plates and enable data from shots to be available in real time.
dHiRes II: This is a high-resolution time resolved x-ray spectrometer utilizing conical crystals to measure line emission from Ar.
DIXI3: "Dilation Imager for X-rays at Ignition". A DIXI high temporal resolution x-ray imager will be mounted at the equator of the NIF target chamber.
FBIT: Full Beam In-Tank (UV intensity at TCC)
Beamlets: Gated Optic Imager to measure relative changes in 60+TOP9 refracted beam intensity (CBET)
T-OPA TBD: Transmitted Beam Diagnostic for the Tunable Optical Parametric Amplifier beam (EP UV beam injected into port P9 on the OMEGA target chamber for LPI studies)
NIF Scattered Light: Fiber-based, compact spectroscopic measurements for SBS and SRS (add ~5 units per year)
FABS: Full Aperture Back Scatter (streaked SBS and SRS)
OTS: Optical Thomson Scattering (5ω is being pursued currently on the NIF with significant
TS: Thomson Scattering
ROSS: Rochester Optical Streak System (camera)
PXTD: Particle and X-ray Temporal Diagnostic (simultaneous proton, neutron and x-ray burn history)
2nd LOS (nTOF): Shielded neutron Time-Of-Flight for simultaneous DD/DT yields, T_{ion} and ρR (via n,T backscatter 10-12 MeV Down Scattered Ratio, DSR)
3D nTOF: 3 axes of antipodal neutron time-of-flight (nTOF)
3rd LOS (nTOF): Third shielded nTOF; challenge is finding a suitable line-of-sight
NIS: Neutron Imaging System (scoping feasibility initially)
KoDI: Knock-on Deuteron Imager (extension of existing Proton Core Imaging System)
CherenTOF: nTOF diagnostic based on a Cherenkov radiator rather than a conventional scintillator
GCD: g-ray Cherenkov Detector (time-integrated and time-resolved versions to be pursued)
SLOS-TRXI: Single Line-of-Sight Time-Resolved X-ray Imager

PXRDP(t): Time-resolved diffraction
XRPHC: X-Ray PinHole Camera
HOTSPEC: Hard x-ray spectrometer to infer electron temperature
Spec-Te: Low energy x-ray spectrometer to infer electron temperature
GXSC: "Generic" X-ray Streak Camera (use existing tubes and modern pulsers, package for use in a TIM, add configuration options)
EXAFSvH: New crystals in existing von Hamos spectrometer for EXAFS measurements of various materials (initially FeO and Fe)
XANES: New crystal(s) in EP High Resolution Spectrometer to measure XANES modulations
3rd LOS GXI: Time-resolved imager (likely a KBFramed front-end with a DIXI readout)
UFXRSC: Ultra-Fast (<ps) X-Ray Streak Camera
ZP: Zone Plates (<few microns resolution x-ray imager)
SCI: Spherical Crystal Imager (updated crystal configurations to image specific lines/ranges)
CCPt: This is a convex crystal spectrometer coupled to an hCMOS camera in the axial diagnostic package. The primary application is time-gated opacity measurements.
Line VISAR: This is 1-D imaging open-beam VISAR system developed in collaboration between SNL and LLNL. The primary application is measuring current delivery to MDD-ICF targets.
HE-diodes: This is a high energy filtered diode array. The primary application is measuring the time-dependent x-ray output spectrum from >15 keV x-ray sources.
CRS: This is a time-integrating spectrometer that measures recoil protons from DD or DT neutrons. The primary application is measuring the burn-averaged neutron spectrum from the stagnation in MDD-ICF.
Gated Backlighting: This is a spherical crystal backlighter coupled to an hCMOS camera. The primary application is measuring the liner mass distribution near stagnation in MDD-ICF.
GRH: This is a gamma reaction history diagnostic to measure the time-history of the DT fusion production in MDD-ICF (requires ~1% tritium on Z).
DT-nImager: This is a time-integrating 2-D neutron imager optimized for primary DT neutrons from the stagnation in MDD-ICF.
MRS: This is a time-integrating spectrometer that measures the recoil protons from DT neutrons. The primary application is measuring the neutron spectrum from the stagnation in MDD-ICF with higher resolution and range than the CRSLocal Diagnostic Efforts on OMEGA

Technical Readiness Levels

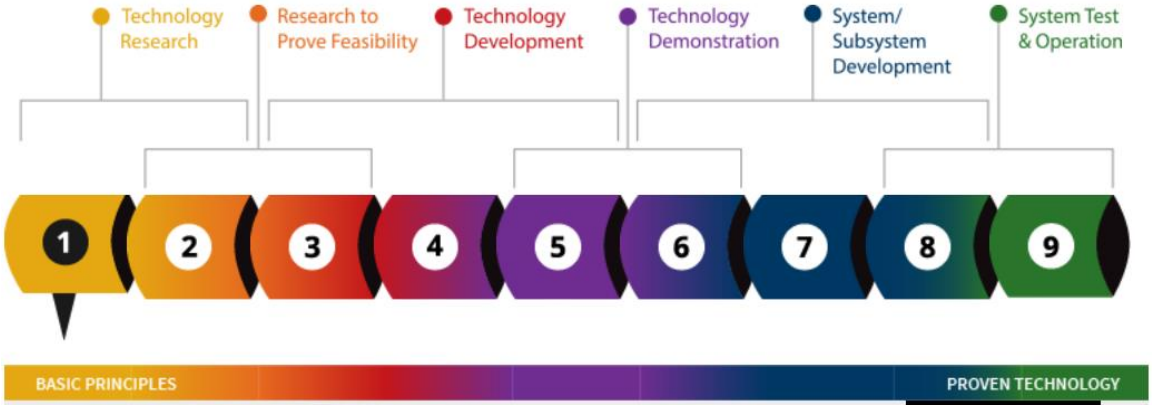

This work was performed under the auspices of the U.S. Department of Energy by Lawrence Livermore National Laboratory under Contract DE-AC52-07NA27344.